

## Comparison and Sensitivity of ODASI Ocean Analyses in the Tropical Pacific

CHAOJIAO SUN

*Global Modeling and Assimilation Office, NASA Goddard Space Flight Center, Greenbelt, and Goddard Earth Sciences and Technology Center, University of Maryland, Baltimore County, Baltimore, Maryland*

MICHELE M. RIENECKER

*Global Modeling and Assimilation Office, NASA Goddard Space Flight Center, Greenbelt, Maryland*

ANTHONY ROSATI, MATTHEW HARRISON, AND ANDREW WITTENBERG

*Geophysical Fluid Dynamics Laboratory, Princeton, New Jersey*

CHRISTIAN L. KEPPELNE, JOSSY P. JACOB, AND ROBIN M. KOVACH

*Global Modeling and Assimilation Office, NASA Goddard Space Flight Center, Greenbelt, and Science Applications International Corporation, Beltsville, Maryland*

(Manuscript received 22 February 2006, in final form 22 September 2006)

### ABSTRACT

Two global ocean analyses from 1993 to 2001 have been generated by the Global Modeling and Assimilation Office (GMAO) and Geophysical Fluid Dynamics Laboratory (GFDL), as part of the Ocean Data Assimilation for Seasonal-to-Interannual Prediction (ODASI) consortium efforts. The ocean general circulation models (OGCM) and assimilation methods in the analyses are different, but the forcing and observations are the same as designed for ODASI experiments. Global expendable bathythermograph and Tropical Atmosphere Ocean (TAO) temperature profile observations are assimilated. The GMAO analysis also assimilates synthetic salinity profiles based on climatological  $T$ - $S$  relationships from observations (denoted "TS scheme"). The quality of the two ocean analyses in the tropical Pacific is examined here. Questions such as the following are addressed: How do different assimilation methods impact the analyses, including ancillary fields such as salinity and currents? Is there a significant difference in interpretation of the variability from different analyses? How does the treatment of salinity impact the analyses? Both GMAO and GFDL analyses reproduce the time mean and variability of the temperature field compared with assimilated TAO temperature data, taking into account the natural variability and representation errors of the assimilated temperature observations. Surface zonal currents at 15 m from the two analyses generally agree with observed climatology. Zonal current profiles from the analyses capture the intensity and variability of the Equatorial Undercurrent (EUC) displayed in the independent acoustic Doppler current profiler data at three TAO moorings across the equatorial Pacific basin. Compared with independent data from TAO servicing cruises, the results show that 1) temperature errors are reduced below the thermocline in both analyses; 2) salinity errors are considerably reduced below the thermocline in the GMAO analysis; and 3) errors in zonal currents from both analyses are comparable. To discern the impact of the forcing and salinity treatment, a sensitivity study is undertaken with the GMAO assimilation system. Additional analyses are produced with a different forcing dataset, and another scheme to modify the salinity field is tested. This second scheme updates salinity at the time of temperature assimilation based on model  $T$ - $S$  relationships (denoted "T scheme"). The results show that both assimilated field (i.e., temperature) and fields that are not directly observed (i.e., salinity and currents) are impacted. Forcing appears to have more impact near the surface (above the core of the EUC), while the salinity treatment is more important below the surface that is directly influenced by forcing. Overall, the TS scheme is more effective than the T scheme in correcting model bias in salinity and improving the current structure. Zonal currents from the GMAO control run where no data are assimilated are as good as the best analysis.

---

*Corresponding author address:* Dr. Chaojiao Sun, Code 610.1, Global Modeling and Assimilation Office, NASA Goddard Space Flight Center, Greenbelt, MD 20771.  
E-mail: chaojiao.sun@gsfc.nasa.gov

DOI: 10.1175/MWR3405.1

© 2007 American Meteorological Society

## 1. Introduction

Ocean data assimilation has reached a level of maturity such that, with ocean observations available in a timely manner, ocean products are now regularly generated for many applications. One important application of ocean data assimilation is the initialization of climate forecasts. The ocean's thermal inertia provides the memory for the climate system at seasonal and longer time scales. The initialization of the ocean state therefore plays a key role in the ability to forecast El Niño with coupled models. To forecast El Niño, the thermal structure in the equatorial Pacific waveguide has to be well represented. Coupled climate forecast systems usually start with ocean initial conditions generated by assimilating subsurface temperature data into an ocean model driven by observed forcing. Alves et al. (2004) show that the sensitivity of forecasts to forcing is much reduced and forecast skills are improved when initial conditions are generated through assimilation, suggesting that the impact of wind error could be mitigated by ocean subsurface data assimilation. In addition to climate forecast initialization, assimilation is also used to synthesize available observations into an analysis of the historical climate record (e.g., Stammer et al. 2002; Carton and Giese 2006, manuscript submitted to *J. Geophys. Res.*).

Approaches to data assimilation vary in degrees of sophistication. The experience in atmospheric assimilation seems to indicate that the effort expended in improving such details as forecast error covariances, model biases, observation representation errors, and the quality control of observations may be more important than the sophistication of the assimilation technique. For the atmosphere, covariance scales are often estimated by analysis of the innovations (observation minus forecast) or from the difference between forecasts and corresponding analyses. Unfortunately, except for sea surface height (SSH) and sea surface temperature (SST), there are so few synoptic observations of ocean fields available that the estimation of forecast error covariances for the ocean is problematic.

Advances seem unlikely beyond the simple structures used by, for example, Behringer et al. (1998) and Rosati et al. (1997), if our estimation of the covariance structure is based on differences between model forecast and observation. One possibility is to use ensembles of ocean simulations (forecasts), which are formed by perturbations of forcing and/or perturbations of internal parameters, to assess the error structures. These error structures then have a dynamical basis for their anisotropy and heterogeneity. Such ensembles have been used by Borovikov et al. (2005) in a

static mode and by Keppenne and Rienecker (2002) in a time-evolving ensemble Kalman filter (EnKF; Evensen 1994, 2003; Keppenne et al. 2005). The question is whether such details impact the analyses and subsequent forecasts with any discernible significance. Here, we use the better exercised systems of optimal interpolation (OI) and three-dimensional variational data assimilation (3DVAR) to address basic questions such as the following: How do different assimilation procedures impact the analyses, including fields such as salinity and currents that are not observed and updated by assimilation? Is there a significant difference in interpretation of the variability from different analyses?

Several studies have shown that salinity can play an important role in the variability of the tropical oceans (e.g., Roemmich et al. 1994; Lukas and Lindstrom 1991). Salinity could influence the stability of the water column and heat buildup in the western equatorial Pacific, and have significant impact on the generation of El Niño and La Niña (Maes et al. 2005). Historically, both subsurface temperature and SSH assimilation have been conducted in a univariate sequential assimilation system (e.g., OI or 3DVAR) where only temperature corrections have been made. The burden has been on the model to modify the salinity and flow fields in accordance with the new temperature analysis. In recent years, evidence has emerged of the potential deleterious effects of univariate sequential assimilation on both temperature and salinity fields and hence on the density field in some assimilation systems (e.g., Ji et al. 2000; Troccoli et al. 2002, 2003; Burgers et al. 2002; Bell et al. 2004). The salinity field can be severely degraded and result in artificially strong convection and vertical mixing when correcting temperature without a concomitant correction in salinity (Derber and Rosati 1989; Troccoli and Haines 1999). The degradation of the mass field then leads to poor flow fields (e.g., Vialard et al. 2003; Ricci et al. 2005).

Given the scarcity of salinity observations, salinity corrections are usually made by reference to the temperature analysis (e.g., Troccoli et al. 2003), by relating altimeter data to temperature and salinity profiles (e.g., Behringer et al. 1998; Segschneider et al. 2001), or by more sophisticated multivariate schemes (e.g., Borovikov et al. 2005; Keppenne et al. 2005). While Segschneider et al. (2001) used altimeter data to provide synthetic temperature and salinity profiles, the increases in 6-month forecast skill appeared to be due primarily to improved correction of salinity rather than to the use of altimeter data per se. Argo profiles of both temperature and salinity to 2000-m depth will likely significantly improve ocean analysis by updating temperature and salinity fields simultaneously.

As part of the Ocean Data Assimilation for Seasonal-to-Interannual Prediction (ODASI) consortium effort, assimilations have been run from 1993 to 2002 by various ODASI members, using the same forcing dataset and observation data streams to facilitate the intercomparison of the results. The ODASI consortium was an activity of the National Oceanic and Atmospheric Administration's (NOAA's) Climate Dynamics/Experimental Prediction (CDEP) program. The consortium was focused toward improving ocean data assimilation methods and their implementation in support of forecasts with coupled general circulation models. The consortium activities were coordinated across four themes: ocean data assimilation product intercomparisons, development of observational data streams; model sensitivity experiments, and validation of assimilation products in forecast experiments. The ultimate goal was to accelerate progress in improving coupled model forecast skill. The main participants were the Center for Ocean-Land-Atmosphere Studies (COLA), International Research Institute for Climate and Society (IRI), The Lamont-Doherty Earth Observatory (LDEO), NOAA's National Centers for Environment Prediction (NCEP), NOAA's Geophysical Fluid Dynamics Laboratory (GFDL), and the Global Modeling and Assimilation Office (GMAO) at the National Aeronautics and Space Administration (NASA) Goddard Space Flight Center.

Here we focus on two global ocean data assimilation systems from GFDL and GMAO. These two systems use different global ocean general circulation models (OGCMs) and different assimilation methods. The purpose of this paper is to evaluate these two analyses from 1993 to 2001 and investigate the importance of salinity treatment. Furthermore, the impact of forcing is explored by sensitivity experiments. Given the end application of interest, namely, seasonal climate forecasts, we focus the evaluation and comparisons on the tropical Pacific.

This paper is organized as follows: the two ocean models used at GMAO and GFDL and datasets of forcing and observations are briefly described in section 2. In section 3, the two ocean data assimilation systems are summarized. The two analyses from GMAO and GFDL are evaluated in section 4. Results from sensitivity experiments are discussed in section 5. We summarize the results and provide conclusions in section 6.

## 2. Ocean models and data

### a. GMAO ocean model

The GMAO ocean model is the Poseidon global OGCM (Schopf and Loughe 1995; Yang et al. 1999). It

is a finite-difference, reduced-gravity ocean model and uses a generalized vertical coordinate designed to represent turbulent, well-mixed surface layers and nearly isopycnal deeper layers. Spherical coordinates with a staggered Arakawa B grid are used in the horizontal. The prognostic variables are layer thickness, temperature, salinity, and current components. The SSH field is diagnostic.

Vertical mixing is parameterized through a Richardson-number-dependent mixing scheme (Pacanowski and Philander 1981) implemented implicitly. An explicit mixed layer is embedded within the surface layers following Sterl and Kattenberg (1994). For layers within the mixed layer, the vertical mixing and diffusion are enhanced to mix the layer properties through the depth of the diagnosed mixed layer. A time-splitting integration scheme is used whereby the hydrodynamics are done with a short time step (15 min), but the vertical diffusion, convective adjustment, and filtering are done with coarser time resolution (half daily). In this study, the global resolution is  $1/3^\circ$  latitude  $\times$   $5/8^\circ$  longitude, with 27 vertical layers.

### b. GFDL ocean model

The GFDL Modular Ocean Model version 4 (MOM4) is a finite-difference version of the ocean primitive equations under the Boussinesq and hydrostatic approximation. Here we summarize some basic information; details are available from Griffies et al. (2005) and Gnanadesikan et al. (2006). It uses spherical coordinates in the horizontal (tripolar grid; see Murray 1996) with a staggered Arakawa B grid and the  $z$  coordinate in the vertical. The ocean surface boundary is computed as an explicit free surface. The meridional resolution varies between  $1^\circ$  in the midlatitudes and  $1/3^\circ$  in the Tropics to resolve the equatorial waveguide. The zonal resolution is  $1^\circ$ . There are 50 vertical levels with 22 uniformly spaced in the upper 220 m. The thickness gradually increases to a value of 366 m at depth. Vertical mixing follows the nonlocal K-profile parameterization (KPP) of Large et al. (1994). The horizontal mixing of tracers uses the isoneutral method pioneered by Gent and McWilliams (1990). The horizontal mixing of momentum uses an anisotropic viscosity scheme that produces large viscosity in the east-west direction, but relatively small viscosity in the north-south direction outside of boundary currents, similar to that of Large et al. (2001).

### c. Forcing and observation data

The common forcing dataset used by the ODASI consortium (denoted "ODASI forcing") includes the

NCEP Climate Data Assimilation System 1 (CDAS 1) daily mean surface fluxes and wind stress [with wind stress climatology replaced by Atlas/Special Sensor Microwave Imager (SSM/I) analyses], and Reynolds SST to provide an additional constraint on SST evolution (Reynolds and Smith 1994; Reynolds et al. 2002).

The observations used in the assimilation are the global expendable bathythermograph temperature profiles available from the National Oceanographic Data Center (NODC) archive, and temperature profiles in Tropical Atmosphere Ocean (TAO)/Triangle Trans-Ocean Buoy Network (TRITON)/Pilot Research Moored Array in the Tropical Atlantic (PIRATA) mooring data (<http://www.pmel.noaa.gov/tao/>; McPhaden et al. 1998) are from the TAO project Web site. Various quality control procedures were implemented to ensure the quality of the data.

### 3. The ocean data assimilation systems

Here we summarize the main characteristics of the GMAO and GFDL ocean data assimilation systems. The main parameters used in the two ocean data assimilation systems are shown in Table 1.

#### a. GMAO ocean data assimilation systems

The GMAO has developed a hierarchy of assimilation systems, from univariate OI (Troccoli et al. 2003) to multivariate OI (Borovikov et al. 2005) to the ensemble Kalman filter (Keppenne et al. 2005). Here the univariate OI scheme used to initialize the GMAO's coupled forecast system is evaluated.

The background-error covariance used in the OI is constant in time. Here the anisotropic Gaussian function depends only on the distance between forecast locations:

$$P^f(\Delta\lambda, \Delta\phi, \Delta z) = C \exp \left[ - \left( \frac{\Delta\lambda}{L_\lambda} \right)^2 - \left( \frac{\Delta\phi}{L_\phi} \right)^2 - \left( \frac{\Delta z}{L_z} \right)^2 \right],$$

where  $L_\lambda$  defines the zonal decorrelation scale,  $L_\phi$  the meridional decorrelation scale, and  $L_z$  the vertical decorrelation scale. In this application,  $L_\lambda = 1800$  km,  $L_\phi = 400$  km in the equatorial waveguide, and  $L_z = 50$  m. The horizontal scales are consistent with those used by Ji et al. (1995). The value for  $L_\lambda$  is modulated meridionally as suggested by Derber and Rosati (1989) to shorten the covariance scales with latitude. For the background error covariance of salinity, the relevant scales are set to  $L_\lambda = 800$  km,  $L_\phi = 300$  km in the equatorial waveguide, and  $L_z = 40$  m. The model error variance is assumed to be homogeneous with a value of  $(0.7^\circ\text{C})^2$ . The observational error variance is assumed

TABLE 1. Main parameters used in the GMAO and GFDL assimilation systems.

	GMAO	GFDL
Assimilation method	OI	3DVAR
Observation temperature error ( $^\circ\text{C}$ )	0.5	0.5
Model temperature error ( $^\circ\text{C}$ )	0.7	0.2
Synthetic salinity observation error	200% of model error	N/A
SSS relaxation time scale (days)	730	10
SST relaxation time scale (days)	10	10

to be  $(0.5^\circ\text{C})^2$  to account for representation error in addition to instrument error. Observation errors are assumed to be white in time and to have a decorrelation scale of 1500 km.

In addition to the temperature data assimilation, the GMAO system uses a separate univariate OI to provide a corresponding salinity analysis. The salinity analysis is based primarily on synthetic salinity profiles derived from the observed temperature profiles and historical  $T$ - $S$  relationships from the Levitus and Boyer (1994) monthly climatologies. We refer to this scheme as the "TS scheme" hereafter. The observational error variance of the synthetic salinity observations is set to 4 times the forecast (or background) error variance. This allows correction of model bias in salinity, yet preserves interannual variability of the salinity field inherent in the model simulation and in the corresponding temperature data.

The assimilation window is 10 days, with data up to 5 days before and 5 days after included with a temporal decay of 20 days applied to the innovations, similar to that of Alves et al. (2004). The assimilation is performed every 5 days.

#### b. GFDL ocean data assimilation system

The GFDL ocean data assimilation system uses the 3DVAR implementation by Derber and Rosati (1989), with background error variance varying geographically (see also Rosati et al. 1997; Zhang et al. 2005). Only temperature profiles are assimilated. The assimilation window is 30 days, using data up to 15 days before and 15 days after the assimilation time. The background error covariance matrix is constructed by multiplying a uniform background variance  $\sigma_b^2$  to an equivalent correlation model (implemented by repeated applications of a Laplacian smoother, using a zonal scale  $x_L$  and a meridional scale  $y_L$ ) as

$$\rho(r_x, r_y) = \exp \left[ - \left( \frac{r_x}{x_L} \right)^2 - \left( \frac{r_y}{y_L} \right)^2 \right],$$

where  $r_x$  and  $r_y$  are the zonal and meridional distance, respectively, of the grid point to the observation location. The elliptic nature of the correlation structure is controlled by  $x_L$  and  $y_L$ . At the equator,  $x_L$  is roughly 700 km and  $y_L$  is 50 km while the correlation structure around 20°N(S) is roughly isotropic (see Zhang et al. 2005). The background error variance,  $\sigma_b^2$ , is set to  $(0.2^\circ\text{C})^2$ . The observational errors are assumed uncorrelated and the error variance is based on the estimate of observed temperature variance, which is set to  $(0.5^\circ\text{C})^2$ .

#### 4. Analysis evaluation and validation

We first compare the temperature field from the GMAO and GFDL analyses with the assimilated TAO temperature profiles at a mooring site as a consistency check. Then, independent data from various sources are compared with the analyses for more rigorous assessment of analysis performance. A simulation-only run (without data assimilation) is also included for comparison: the GMAO control run (denoted “GMAO-CTL”). Note that the GMAO-CTL uses a different forcing (the same forcing used in the GMAO seasonal forecast system; denoted “GMAO forcing”) from the ODASI forcing used in the GMAO and GFDL analyses. The comparison of the analyses with the control here is therefore qualitative. However, we will compare the GMAO-CTL with analyses that use both forcings in section 5 to address the role of forcing.

##### a. Comparison with TAO temperature profiles at 140°W

Here we compare the GMAO and GFDL temperature analyses at a mooring location in the equatorial central Pacific with the assimilated TAO profiles. Figure 1 shows the temperature time series from the analyses and TAO observations at 140°W on the equator over the 9-yr period (1993–2001). Both GMAO and GFDL analyses agree well with the TAO observations as expected. The GMAO-CTL exhibits the observed interannual variability and the big warming event during the 1997/98 El Niño. However, it fails to capture the rapid cooling event in the thermocline during the 1998 La Niña (e.g., see the 20° and 16°C isotherms). This is not because GMAO-CTL uses a different forcing dataset, since other GMAO analyses using the same forcing capture this cooling event successfully (not shown).

The statistics of the analyses and observations are shown in Fig. 2. The time mean of the error (difference with TAO temperature) is around 1°C (GMAO) and 0.7°C (GFDL) in the area of the Equatorial Undercur-

rent (EUC), with a standard deviation (STD) of error about 0.8°C (GMAO) and 1.2°C (GFDL). To evaluate the significance of these differences, we compare collocated conductivity–temperature–depth (CTD) and TAO measurements that are within 0.2° radius of each other (as done by Borovikov 2005). The statistics are averaged over northern and southern areas of Niño-3 (5°S–5°N, 150°–90°W) and Niño-4 (5°S–5°N, 160°E to 150°W), to account for the different characteristics of these areas (Fig. 3). The differences of collocated CTD and TAO reach 1°C in the EUC and about 0.2°C below (Fig. 4). If we interpret these differences as the representation error, we may conclude that the differences between each analysis and TAO observation are comparable to representation errors. The variability, represented by the standard deviation of the temperature time series, is captured well in the two analyses, although the peak variability is slightly underestimated.

##### b. Comparison with Reverdin and OSCAR surface current climatology

The surface current estimates in the tropical Pacific are influenced primarily by the surface wind forcing. For example, Fevrier et al. (2000) compared 15-m zonal current anomalies and thermocline depth anomalies in the tropical Pacific from three OGCMs forced by different wind stress products and found that the surface current depends strongly on the wind forcing product; however, parameterizations in surface layer physics also need to be improved to reduce the uncertainty in surface current estimates. Because of the role of advection in SST variations (e.g., Borovikov et al. 2001), it is also of interest whether the assimilation of the temperature profile data impacts the surface current estimate. Unfortunately, few surface current measurements exist. The near-surface estimates from acoustic Doppler current profiler (ADCP) at the TAO moorings are not without error (e.g., Harrison et al. 2001), and the use of drifter estimates requires judicious interpolation and smoothing to produce a time series useful for comparison with the assimilation fields.

Here (Fig. 5) we compare climatologies of the zonal current from GFDL and GMAO analyses with the Reverdin et al. (1994) and Ocean Surface Current Analyses—Real time (OSCAR) climatologies (Lagerloef et al. 1999; Bonjean and Lagerloef 2002). It should be noted that the Reverdin climatology was computed over the 1987–92 period whereas the other climatologies are computed over the 1993–2001 period. The agreement between observations and analyses are generally good. The seasonal variability of the current system, with an intense North Equatorial Counter Current (NECC) near 7°N in boreal fall and weak South Equa-

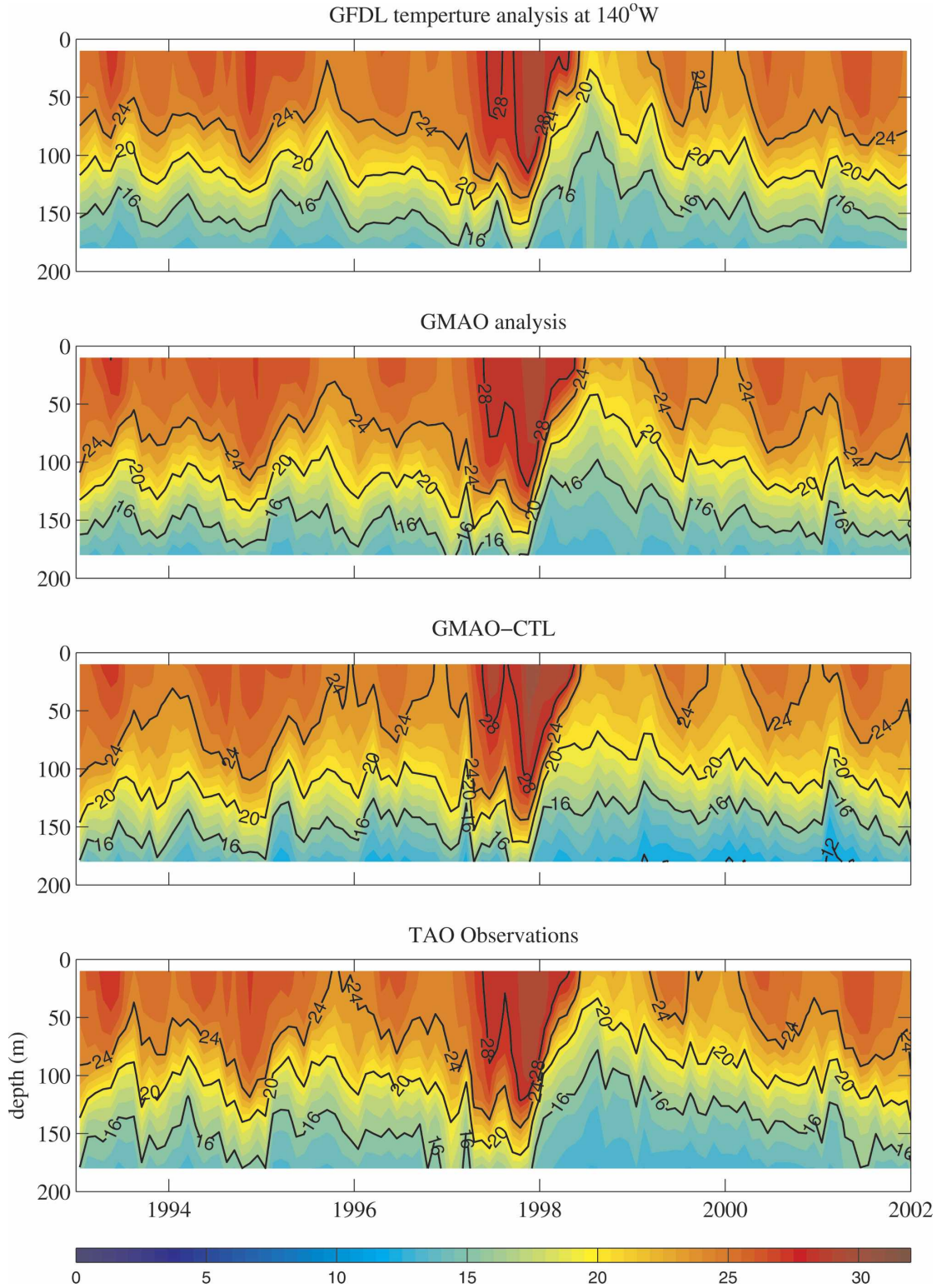
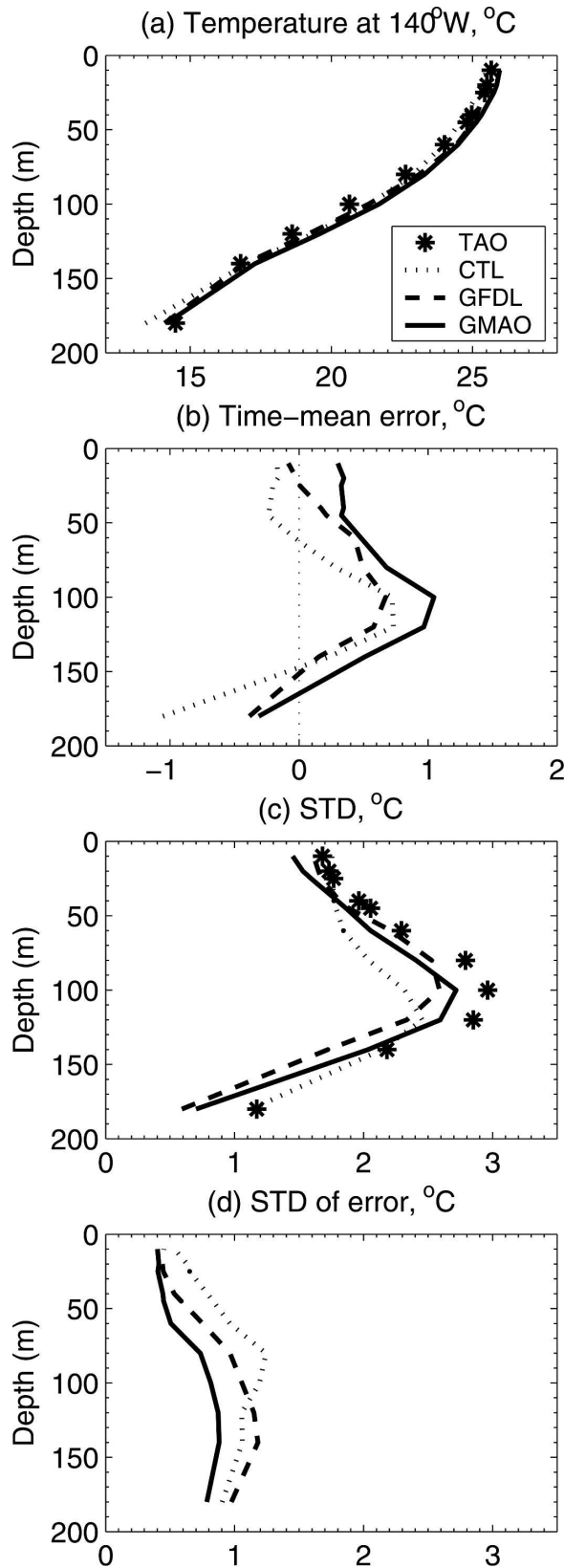


FIG. 1. Time series of temperature from TAO observations and model simulations (1993–2001) at 140°W on the equator. Model results are from the GMAO and GFDL analyses and a control run from GMAO model simulation under the “GMAO forcing.” The model values have been sampled in the same way as the data (no model values are used when the corresponding data are missing).



torial Current (SEC) in spring is present in all the climatologies, as are the off-equatorial double maxima in the SEC. However, the analyses also display some biases. In the GFDL analysis, the western section of the SEC is too strong during summer and fall, and the EUC has surfaced during all seasons. In the GMAO analysis, both the SEC and the NECC are too strong along the western boundary and the surfaced EUC is slightly too strong during summer and fall. The extension of the period of eastward surface flow is not a deficiency of the models [see the GMAO-CTL in Fig. 6 and the results of Harrison et al. (2001), using a similar model as GFDL], but apparently of the assimilation. Even with the same wind forcing (ODASI forcing), there are differences between the GMAO and GFDL surface current analysis estimates. It is noted that the OSCAR product, showing eastward flow throughout the year at the western equatorial boundary, is inconsistent with the other estimates.

Pattern correlations (Tables 2 and 3) show most consistent agreements among the products in fall when the currents are strong and least consistent in spring when the currents are weak. The assimilation products agree equally well with Reverdin and OSCAR in the summer, but better with OSCAR in the other seasons. The GMAO analysis agrees best with the OSCAR product in winter and spring, while the GFDL analysis is in best agreement in summer. The two analyses are in better agreement with each other than with either dataset.

### c. Comparison with TAO ADCP current profiles

Here we compare zonal current analyses with independent current data from ADCPs deployed at three equatorial TAO moorings on the western (165°E), central (140°W), and eastern Pacific (110°W). For reference, GMAO-CTL is also included in the comparisons. Figure 6 shows the time series of GFDL, GMAO, GMAO-CTL, and TAO zonal current from 1993 to 2001. At 165°E in the western equatorial Pacific, both analyses have difficulty with the unusually strong and shallow EUC right after the 1997/98 El Niño, while the GMAO-CTL captures this strong event successfully, although it tends to be too strong in other years. The

←

FIG. 2. Statistics of analyses and control with respect to the equatorial TAO temperature data at 140°W, averaged over 1993–2001: (a) time-mean temperature profiles of TAO, GMAO-CTL, GFDL, and GMAO analyses; (b) time-mean error with respect to TAO; (c) STD of these monthly time series; and (d) STD of error (difference with respect to TAO). The model values have been sampled in the same way as the data (no model values are used when the corresponding data are missing).

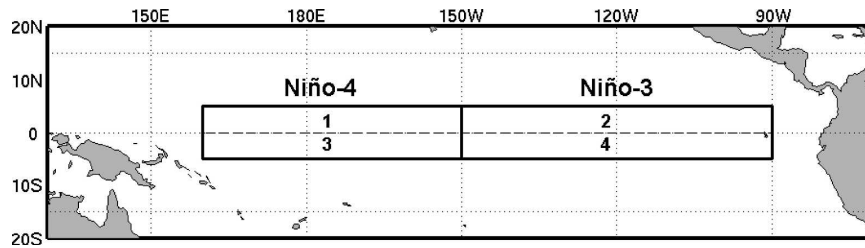


FIG. 3. The four areas for which the RMSD statistics are computed. Areas 1 and 2 are the northern part of the Niño-4 ( $5^{\circ}\text{S}$  to  $5^{\circ}\text{N}$ ,  $160^{\circ}\text{E}$  to  $150^{\circ}\text{W}$ ) and Niño-3 ( $5^{\circ}\text{S}$  to  $5^{\circ}\text{N}$ ,  $150^{\circ}$  to  $90^{\circ}\text{W}$ ) regions; areas 3 and 4 are the southern part of the Niño-4 and Niño-3 regions.

GMAO zonal current has about the right variability; however, the GFDL zonal current is generally too weak. At  $140^{\circ}\text{W}$ , both the GMAO analysis and GMAO-CTL display the observed variability and EUC intensity. The current reversal during the 1997/98 El Niño event is best represented in the control simulation. The GFDL analysis captures the observed structure but the EUC is too shallow. At  $110^{\circ}\text{W}$ , both analyses are able to reproduce the zonal current structure well. The control has difficulty in reproducing the observed EUC intensity.

The statistics of the zonal current profiles averaged over the 9-yr period (1993–2001) are shown in Fig. 7. At  $165^{\circ}\text{E}$ , the time mean of both GFDL and GMAO currents match TAO observations well above 150 m, yet they are both too weak in the EUC region below 150 m. The control run matches the lower part of EUC (below 180 m) very well, but it is too strong elsewhere (up to  $0.20\text{ m s}^{-1}$ ). The variability in all the analyses and control (shown by STD) are similar to the TAO currents, and the standard deviations of their errors are comparable. At  $140^{\circ}\text{W}$ , both the GMAO analysis and GMAO-CTL capture the observed time-mean current structure very accurately. Below 80 m, the GFDL current has a strong westward bias (up to  $0.35\text{ m s}^{-1}$ ). At  $110^{\circ}\text{W}$ , the control current is far too weak above 120 m and thus fails to capture the maximum of the EUC. In section 5, it is shown that two other analyses produced by GMAO using the same forcing as the control have similar current structure at this location. The GFDL and GMAO currents are much closer to the TAO current in that area, although they both have biases below 100 m (a westward bias in the GFDL analysis and an eastward bias in the GMAO analysis). At all three locations, the STD of error is lowest for the control, suggesting that the error in the control current is mainly a bias.

#### d. Comparison with TAO salinity profiles at $156^{\circ}\text{E}$

There are few salinity observations available in the ocean to provide an adequate evaluation of the ocean

analyses. Here we compare our assimilation results with independent salinity data retrieved at an equatorial TAO moored array at  $156^{\circ}\text{E}$  (Fig. 8). The data have undergone quality control based on the quality flags, and obvious outliers are removed before comparison. Near the surface (above 50 m), both analyses tend to be more saline than the observations and they are generally in better agreement with each other than with the observations, probably due to the fact that salinity variations in the tropical Pacific are mainly driven by evaporation minus precipitation ( $E - P$ ) forcing. Below 100 m, the GMAO salinity analysis is much closer to the TAO observation than the GFDL analysis, suggesting that the assimilation of climatological salinity in the GMAO analysis helps to reduce salinity bias in the model.

#### e. Comparison with TAO servicing cruises data

For years, the TAO servicing cruises have collected CTD profiles and subsurface current measurements using shipboard ADCPs during transects to and from the TAO mooring sites (Johnson et al. 2000, 2002). This dataset offers simultaneous measurements of temperature, salinity, and currents. Here we compare our analyses with a gridded analysis of these independent data from 1994 to 1998 (Johnson et al. 2000). Comparison statistics are grouped separately for the northern and southern areas of Niño-3 and Niño-4 regions as defined in Fig. 3. The RMS difference (RMSD) between collocated model and cruise data in these four areas is shown in Fig. 9.

Both analyses generally improve the temperature field over the control, particularly between about 200 and 500 m. As Borovikov et al. (2005) show, the remnant RMS error in the monthly mean comparisons is greater than the higher-frequency variance in the control or in the TAO moorings, so the remaining differences are not likely due to a comparison of asynoptic “snapshots” from the cruises with monthly mean analyses.

The GMAO analysis is generally effective in correct-

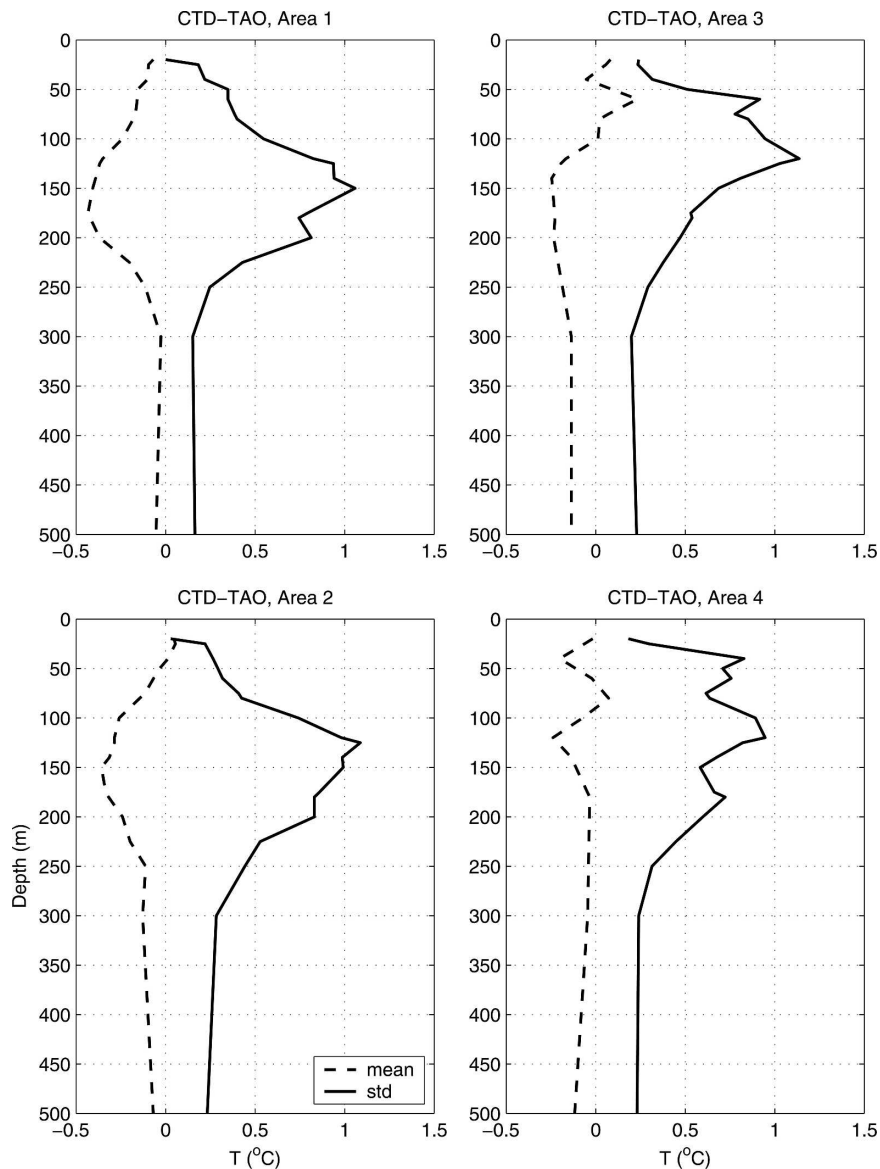


FIG. 4. STD (solid) and time mean (dashed) of the difference in collocated CTD and TAO measurements for the (upper) northern and (lower) southern areas of (right) Niño-3 and (left) Niño-4 regions. The CTD measurements are from TAO servicing cruises conducted during December 1986 to December 1999. The TAO measurements are from the TAO moorings that are collocated with the CTD casts. The collocation requirement is that the measurements were taken within  $\pm 0.2^\circ$  lat and lon and on the same date. The number of profiles in each area is 59 (57) in the Niño-3 region north (south) of the equator and 84 (72) in the Niño-4 region north (south) of the equator.

ing model salinity error, especially in the northern areas of Niño-3 and Niño-4 (areas 1 and 2). In contrast, the GFDL analysis, which does not treat salinity explicitly, has large salinity error in all areas, with the largest near 1 psu in the southern Niño-4 region (area 3). Note that the degradation of the GMAO salinity analysis near surface, most apparent in the southern sections, is due to the inappropriate use of the synthetic salinity data

within the mixed layer. Johnson et al. (2000) show that the isohaline layers in some of these CTD sections extend to below 100 m, which are unlike the climatology used for the synthetic salinity.

The errors in zonal currents from the two analyses and control are comparable except in the southern Niño-4 region (area 3), where the GFDL current has slightly larger error below the thermocline. The fact

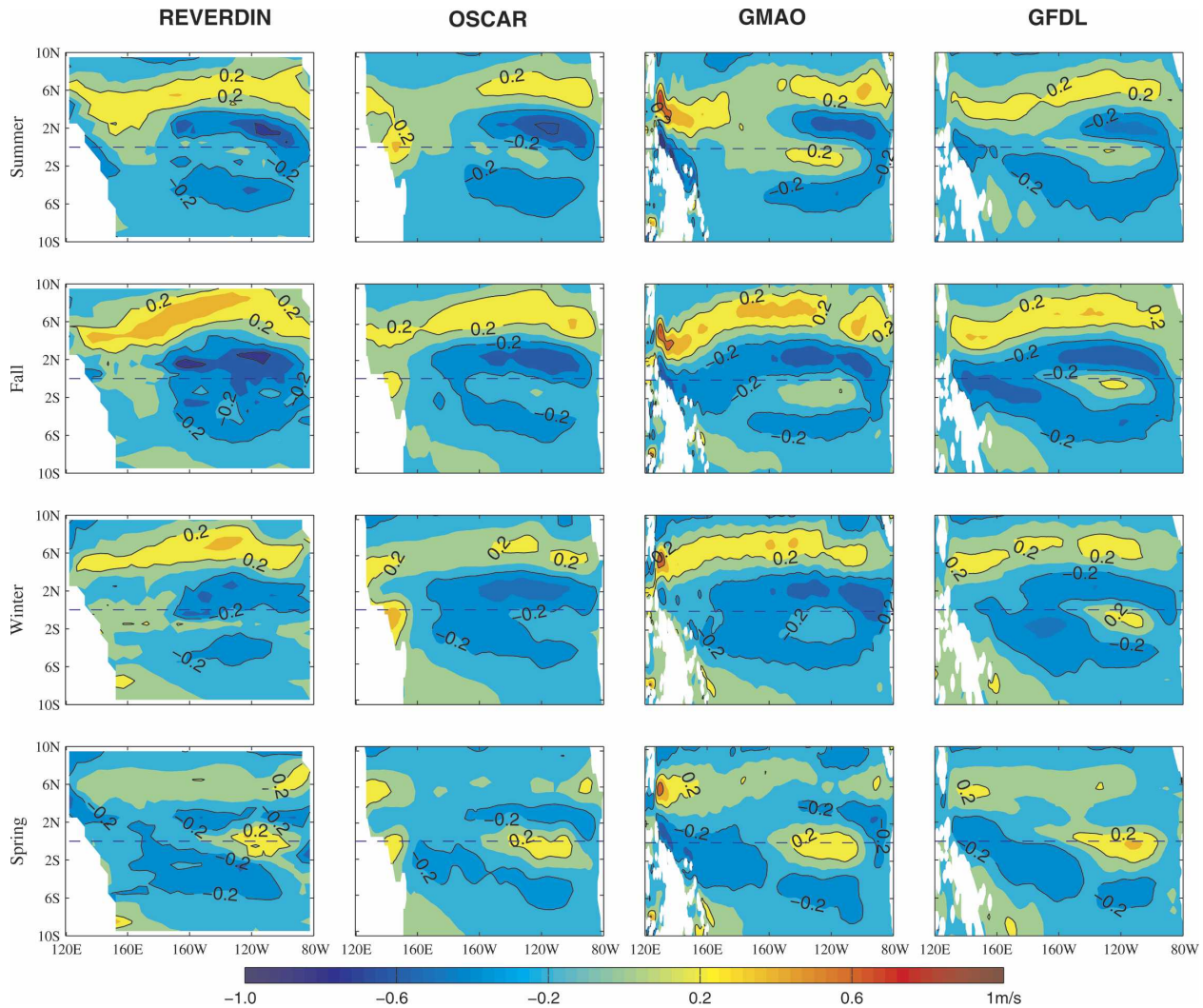


FIG. 5. Seasonal climatology of 15-m zonal current from Reverdin et al. (1994), OSCAR, GMAO, and GFDL analyses. The Reverdin climatology is representative of the period from January 1987 to April 1992. The dashed blue line indicates the equator. (top to bottom) Summer, fall, winter, and spring.

that the control currents are as good as or even slightly better than analysis currents (but not in area 1) is a common phenomenon in ocean analysis systems when only temperature data are assimilated. There could be several reasons. One is that the tropical Pacific is mainly wind driven, and both models are well tuned to simulate the current structure well without assimilation. The assimilation of temperature introduces an imbalance in the model, and a correction is needed to bring the model back to geostrophic balance (e.g., Burgers et al. 2002; Bell et al. 2004; Ricci et al. 2005). Another reason that the control is slightly better than the GMAO analysis current is hinted in the next section: the TS-scheme analysis using the same GMAO forcing as the control produces as good currents as the control. We elaborate further in section 5b.

### 5. Sensitivity analysis

In ocean state estimation, data assimilation helps to compensate for errors in the surface forcing fields as well as the initial conditions. We have seen from the previous section that even with the same forcing fields and observation dataset, there are differences in the ocean analyses generated with different models and assimilation methods. Here we explore the sensitivity of the analysis to the choice of forcing data. Given the importance of correcting salinity during temperature-only assimilation, we also explore the sensitivity of the analysis to the method of salinity correction. These sensitivity experiments are performed with the GMAO assimilation system.

The second set of forcing (i.e., GMAO forcing) is

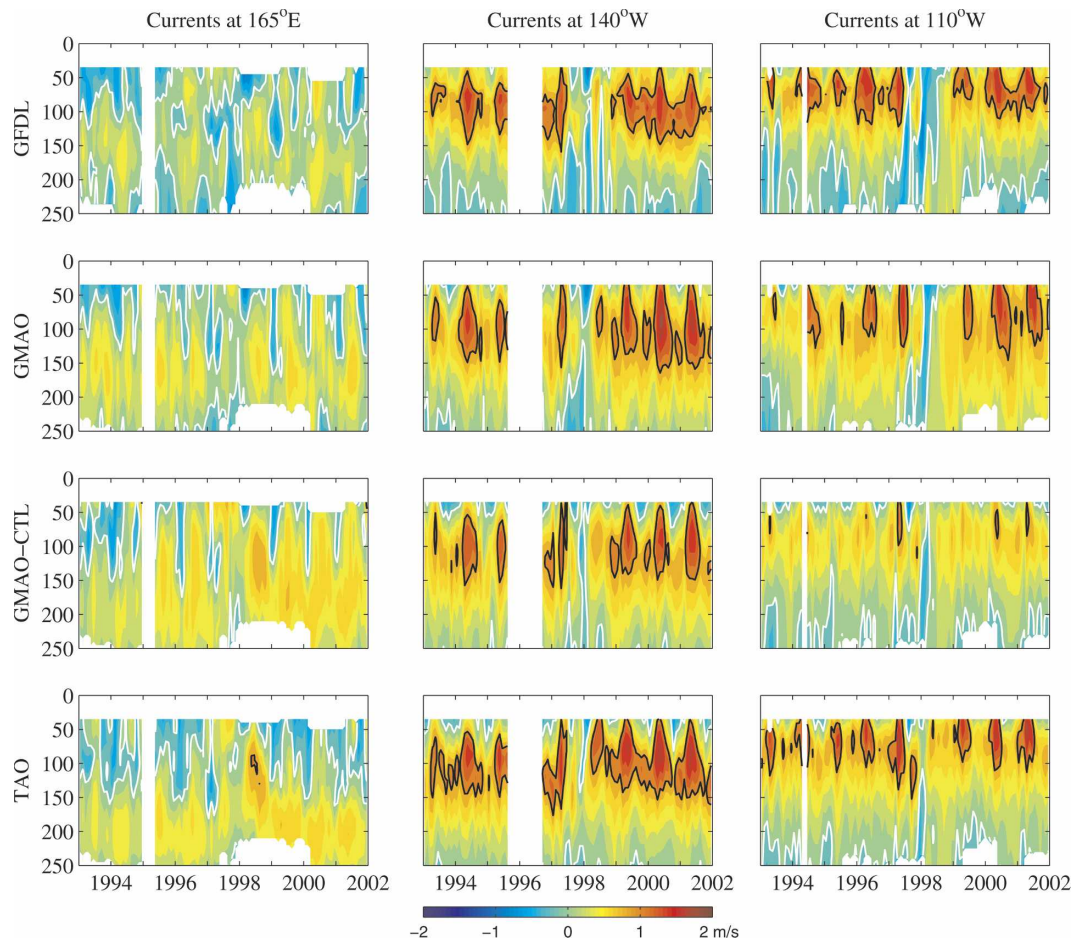


FIG. 6. The time series of zonal current at  $165^{\circ}\text{E}$ ,  $140^{\circ}\text{W}$ , and  $110^{\circ}\text{W}$  on the equator as a function of depth (m) from the TAO observations and models (the GFDL and GMAO analyses, and the GMAO-CTL). The white line is the zero contour line and the black line is the  $1\text{ m s}^{-1}$  contour line. The model values are sampled in the same way as the data (i.e., no model values are used when the corresponding data are missing).

that used in the ocean initialization for the GMAO coupled model forecasts (e.g., Vintzileos et al. 2003, 2005). The forcing comprises SSM/I-derived time-varying wind stress (Atlas et al. 1996), Global Precipitation Climatology Project (GPCP) monthly mean precipitation (Adler et al. 2003), NCEP CDAS 1 short-wave radiation (for penetrating radiation) and latent

heat flux (for evaporation), and Reynolds and Smith (1994) weekly SST. A comparison of zonal wind stress and freshwater flux ( $E - P$ ) from ODASI forcing with those of GMAO forcing at the equator over the 1993–2001 time period is shown in Fig. 10. The seasonal and interannual variations in the two datasets are consistent. However, GMAO zonal wind is often stronger

TABLE 2. Summer/fall seasonal climatology pattern correlations of Reverdin, OSCAR, GMAO, and GFDL analyses. Note that the correlations above the diagonal are for the summer season, and the correlations below the diagonal are for the fall season.

	Reverdin	OSCAR	GMAO	GFDL
Reverdin	1.0000	0.8243	0.7235	0.7946
OSCAR	0.8455	1.0000	0.7532	0.7497
GMAO	0.7412	0.8510	1.0000	0.7838
GFDL	0.7300	0.8250	0.8887	1.0000

TABLE 3. Winter/spring seasonal climatology pattern correlations of Reverdin, OSCAR, GMAO, and GFDL analyses. Note that the correlations above the diagonal are for the winter season, and the correlations below the diagonal are for the spring season.

	Reverdin	OSCAR	GMAO	GFDL
Reverdin	1.0000	0.7787	0.7647	0.6655
OSCAR	0.6224	1.0000	0.8406	0.7823
GMAO	0.6017	0.7455	1.0000	0.8399
GFDL	0.6274	0.6476	0.7560	1.0000

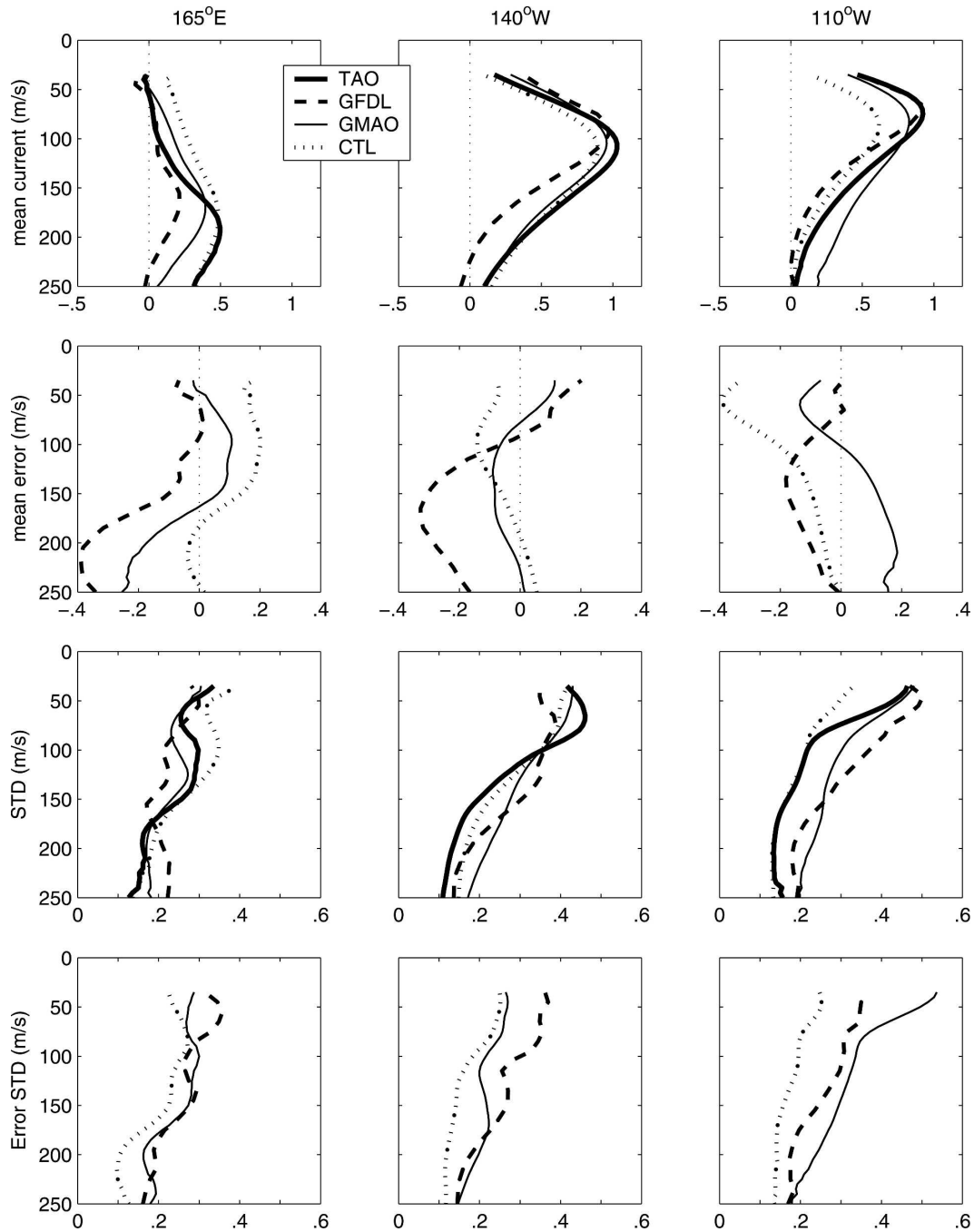


FIG. 7. Statistics of the zonal currents as a function of depth (m) at (left column) 165°E, (middle column) 140°W, and (right column) 110°W on the equator: TAO ADCPs (thick solid curve), GFDL (dashed curve), GMAO (solid curve), and GMAO-CTL (dotted curve). (top) Mean vertical profiles; (second row) mean error as compared to TAO data; (third row) STD of zonal current; and (bottom) STD of error with respect to TAO data. This figure is based on monthly averages over the 9-yr period from 1993 to 2001, with the model values sampled in the same way as the data (no model values are used when the corresponding data are missing).

than the ODASI zonal wind, while  $E - P$  of ODASI forcing is stronger than that of GMAO forcing.

The alternative salinity correction scheme employed is that of Troccoli and Haines (1999): after the subsur-

face temperature data are assimilated, the model salinity field is updated at the analysis time based on the local model  $T-S$  relations to maintain convective stability. We will refer to this scheme as the “T scheme”

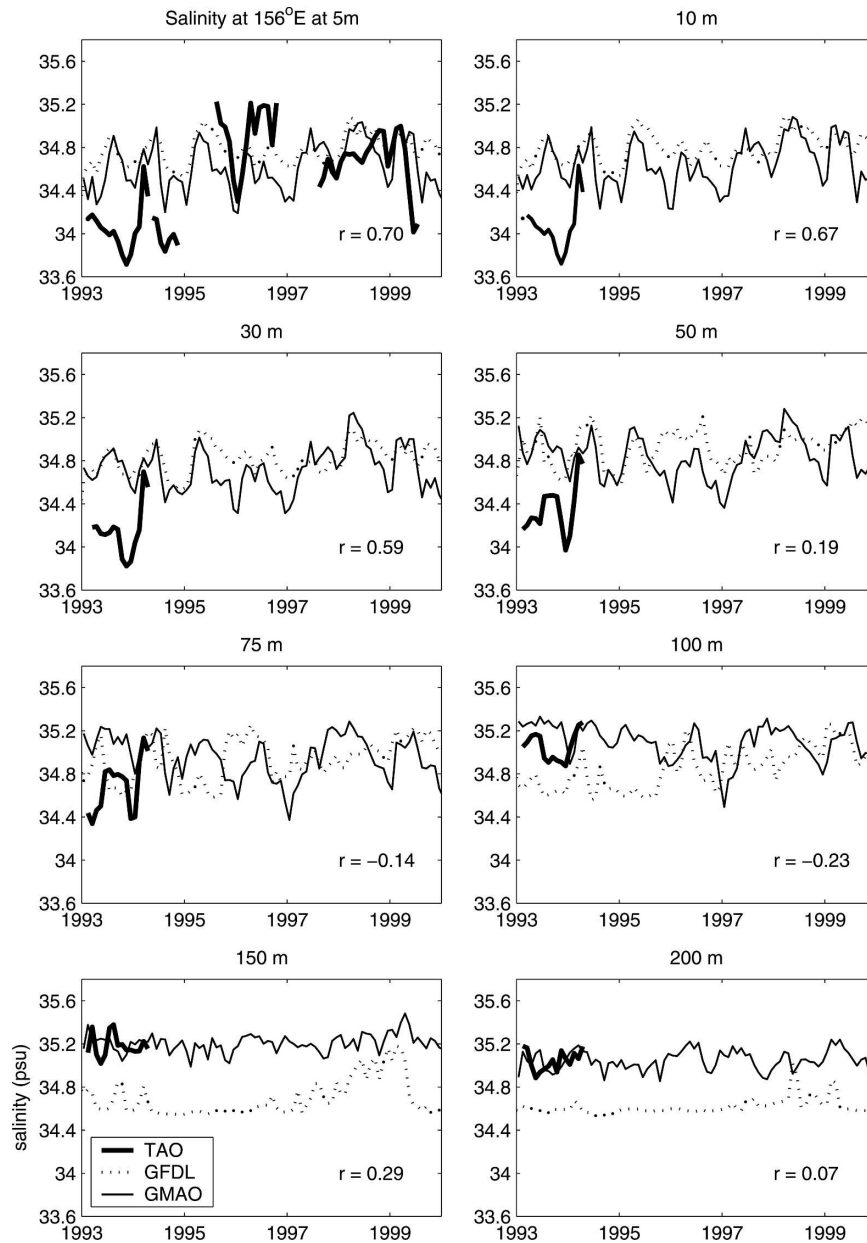


FIG. 8. Time series of monthly mean salinity time series at 156°E on the equator from TAO observations, GFDL, and GMAO analyses. The correlations between the GFDL and GMAO analyses are displayed at the lower right-hand corner of each panel.

hereafter. There is no assimilation in the top layer; the model SST is relaxed to the Reynolds and Smith (1994) weekly SST product, with a seasonally and spatially varying relaxation time scale derived from Comprehensive Ocean–Atmosphere Data Set (COADS) data. Surface salinity is relaxed to Levitus and Boyer (1994) climatology with an  $e$ -folding decay time scale of 2 yr. Salinity within the mixed layer is not updated in this T scheme.

The GMAO experiments evaluated here are denoted

GMAO-T and GMAO-TS for the experiments using GMAO forcing, and ODASI-T and ODASI-TS (this is the GMAO analysis used in comparison with GFDL analysis in the previous section) for the experiments using ODASI forcing (see Table 4). GMAO-CTL is included for comparison.

#### a. Comparison with TAO temperature profiles at 140°W

Here we compare GMAO temperature analyses with dependent data from the TAO mooring at 140°W on

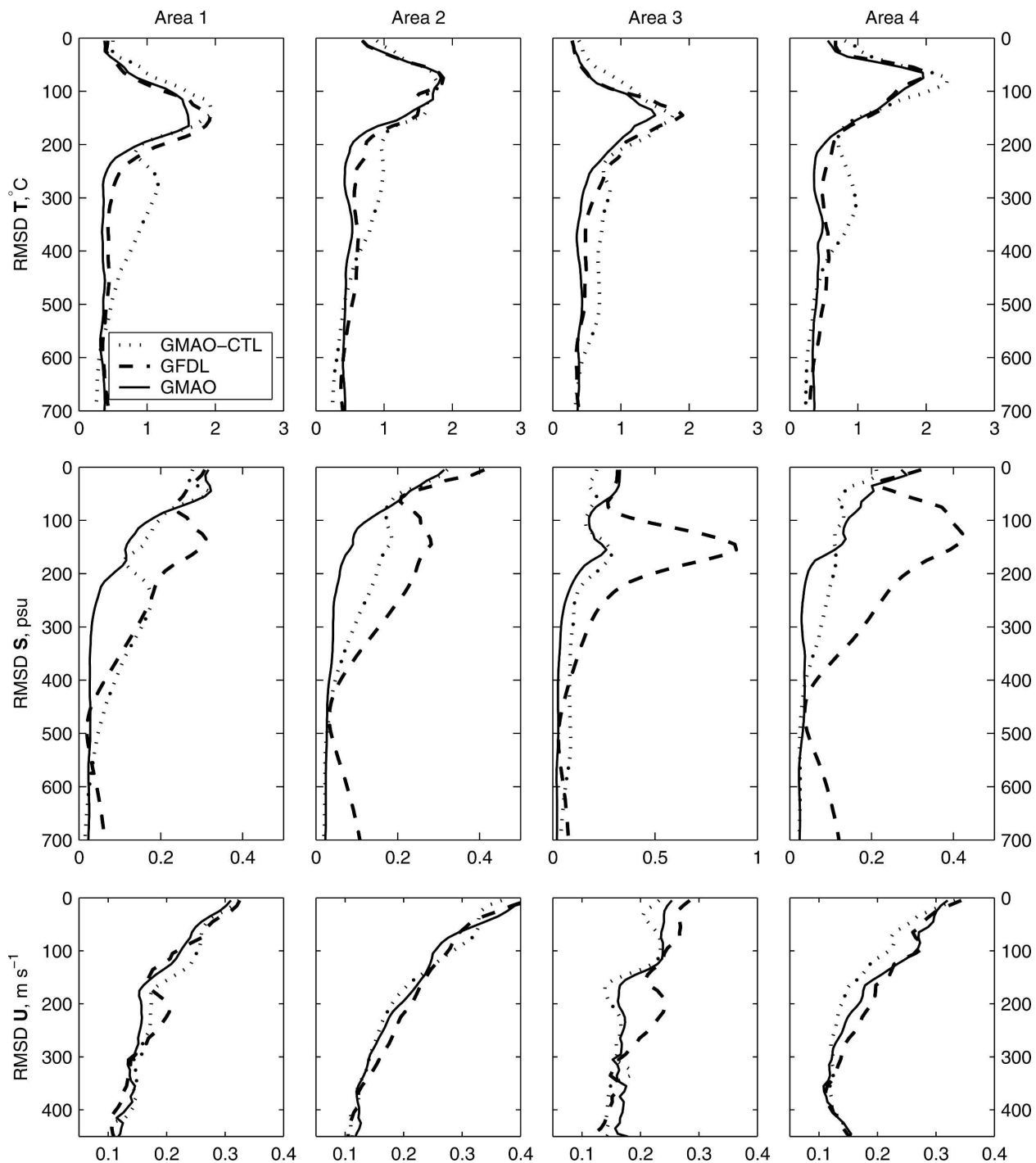


FIG. 9. RMSD of (top) temperature, (middle) salinity, and (bottom) zonal current between each of the model runs (GFDL analysis, GMAO control, and analyses) and observations from TAO servicing cruises (for the 5-yr period 1994–98) as a function of depth (m), averaged over the northern and southern Niño-3 and Niño-4 regions as defined in Fig. 3. Note that the x-axis scale for salinity in area 3 is from 0 to 1 psu, and is twice as large as the scale for the other areas.

the equator (Fig. 11, similar to Fig. 2), similar to section 4a. The mean temperature profiles from the GMAO analyses (averaged over the 9-yr period from 1993 to 2001) agree with the TAO observation (Fig. 11a). How-

ever, they are slightly too warm in the thermocline. Both TS experiments have slightly larger biases than the corresponding T experiments (Fig. 11b). This is not surprising since the assimilation of synthetic salinity in

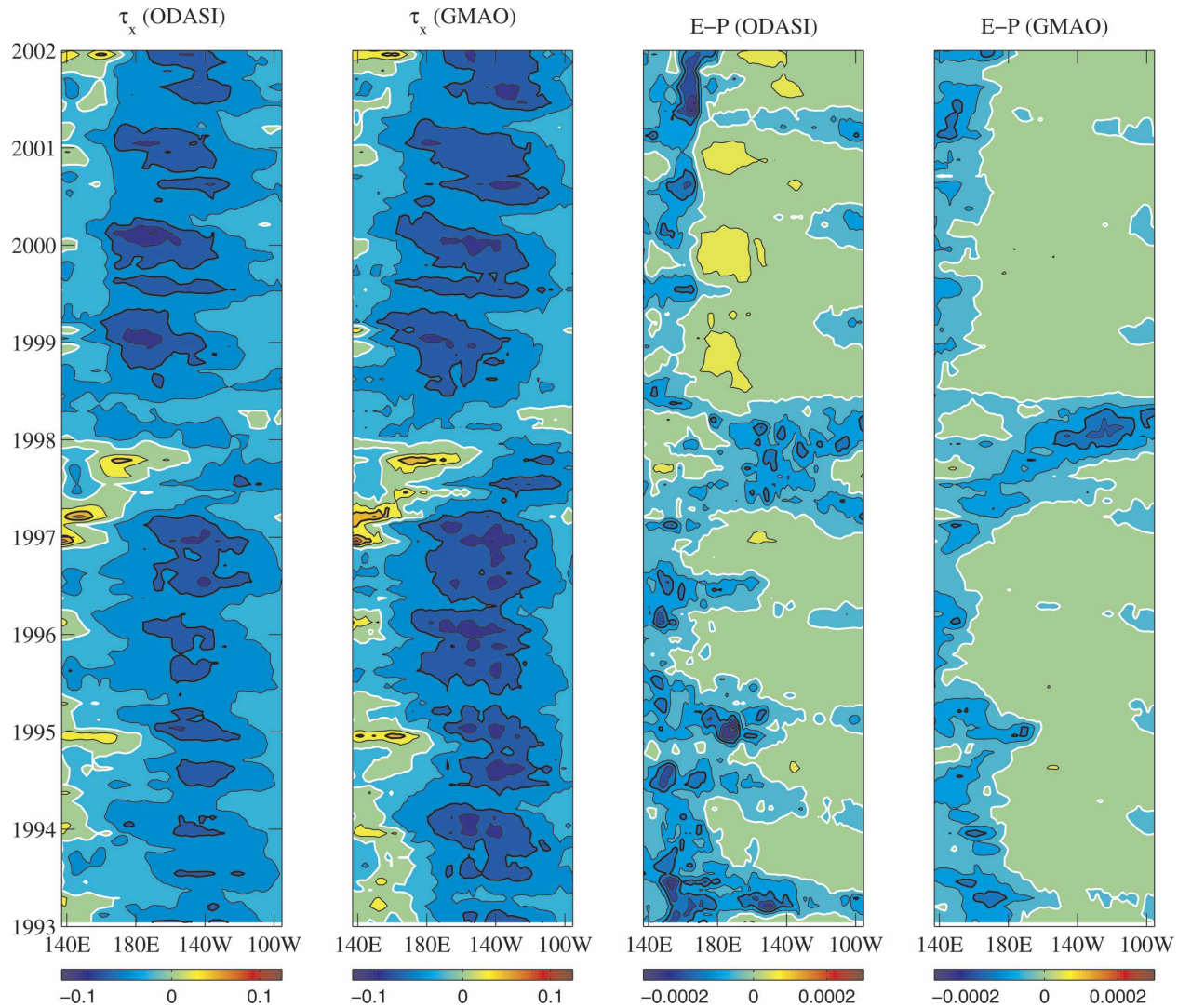


FIG. 10. Comparison of GMAO and ODASI forcing at the equatorial Pacific (140°E to 100°W) from 1993 to 2002. (a) ODASI zonal wind stress ( $\text{N m}^{-2}$ ); (b) GMAO zonal wind stress ( $\text{N m}^{-2}$ ); (c) ODASI freshwater flux,  $E - P$  ( $\text{mm day}^{-1}$ ); and (d) GMAO freshwater flux,  $E - P$  ( $\text{mm day}^{-1}$ ).

TS experiments could cause the analysis to deviate from the model temperature structure. All analyses capture the temporal variability well, with only a slight underestimation of the peak variability (Fig. 11c). The

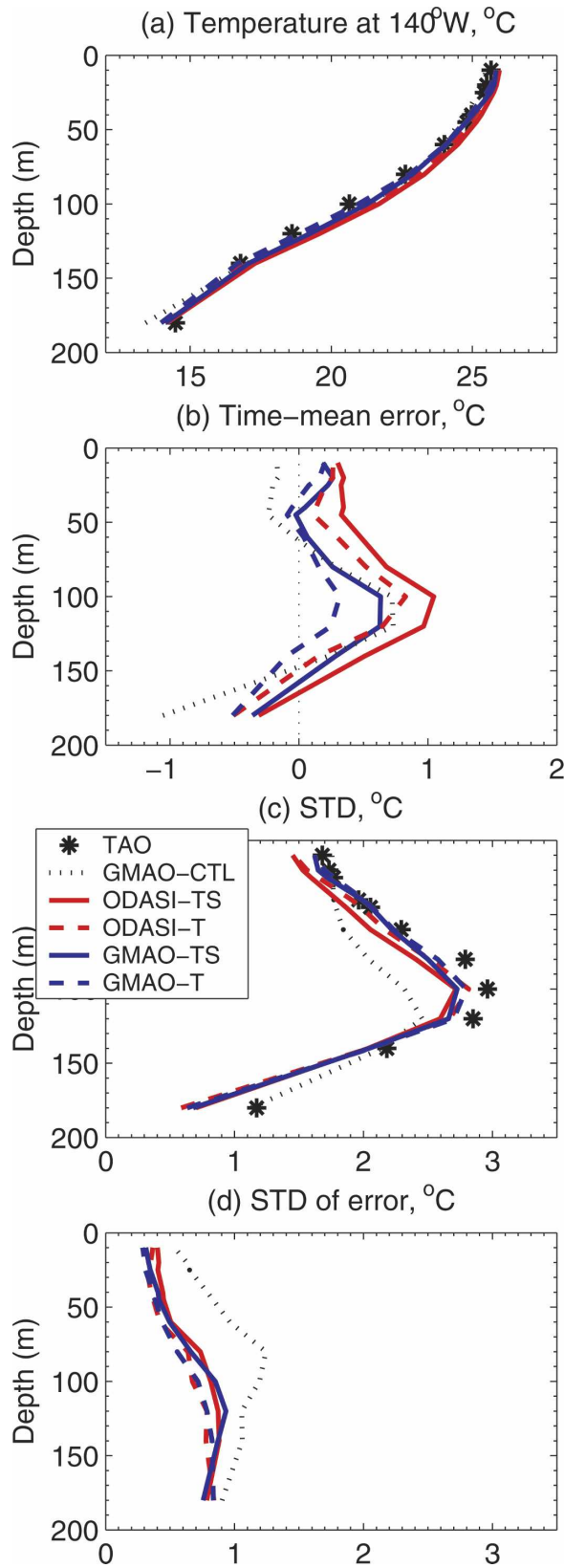
TABLE 4. Summary of experiments.

Expt	Assimilation method	Forcing
GFDL	3DVAR, assimilating $T$ only	ODASI
ODASI-T	OI, assimilating $T$ only	ODASI
ODASI-TS	OI, assimilating $T$ and $S$	ODASI
GMAO-T	OI, assimilating $T$ only	GMAO
GMAO-TS	OI, assimilating $T$ and $S$	GMAO
GMAO-CTL	No assimilation	GMAO

control underestimates the variability in the upper thermocline (above 120 m) and has the largest error STD. The standard deviations of differences are similar for all analyses (Fig. 11d). The GMAO analysis system employs incremental adjustment of the model's ocean state through incremental analysis update (IAU; Bloom et al. 1996). This, in combination with the drift of the model forecast between analysis times, could lead to RMS errors larger than the a priori error estimates for the background and observations.

#### b. Comparison with TAO ADCP current profiles

Similar to section 4c, the GMAO current analyses are compared with independent ADCP observations



made at three TAO moorings on the equator: 140°W, 110°W, and 165°E (Fig. 12, similar to Fig. 7). In the central and eastern equatorial Pacific (140° and 110°W), we find that the mean current above the EUC core from GMAO analyses is mostly influenced by forcing rather than the treatment of salinity (Fig. 12, middle and right columns): the biases from analyses using the same forcing are similar. Below the EUC core, the biases from analyses using the same salinity update scheme are similar, with the TS scheme having smaller biases. The assimilation of climatological salinity effectively reduces the eastward bias below the EUC core present in the two T-scheme analyses. This suggests that the role of forcing becomes less important below the undercurrent core. In the western equatorial Pacific (165°E), the current structure appears to be more sensitive to the salinity treatment in the analyses than the forcing used (Fig. 12, left). The two analyses using the TS scheme have smaller mean error than the other two analyses using the T scheme. However, below about 160 m, the westward bias in the TS analyses is slightly larger than that in the control and T analyses. The reason for this result is not clear.

In summary, there is an overall good agreement among the analyses, control, and TAO current observations. The TS scheme generally produces similar currents to the T scheme under the same forcing in the surface (above the undercurrent core). However, deeper currents from the TS scheme tend to improve upon those from the T scheme, regardless of the forcing used, according to both mean and RMS error measures (except in the western Pacific). This seems to indicate that forcing is the dominant factor in determining the direction and magnitude of the near-surface currents (above 150 m or so), while the salinity treatment has strong impact on the deeper currents. The zonal current from the GMAO control run is too weak in the undercurrent core (except at 165°E), but it is closer to the TAO observations below the core. Interestingly, each analysis tends to degrade the zonal current below the undercurrent core.

The results are consistent with the suggestion of Vialard et al. (2003) and Ricci et al. (2005), who found that the model bias in the salinity from the T scheme

←

FIG. 11. Statistics of GMAO analyses and CTL compared with the equatorial TAO temperature data at 140°W: (a) Climatological temperature profiles of TAO, GMAO control, and GMAO analyses, averaged over 1993–2001; (b) mean error of analyses and CTL with respect to TAO; (c) STD of the temperature monthly time series; and (d) STD of error with respect to TAO.

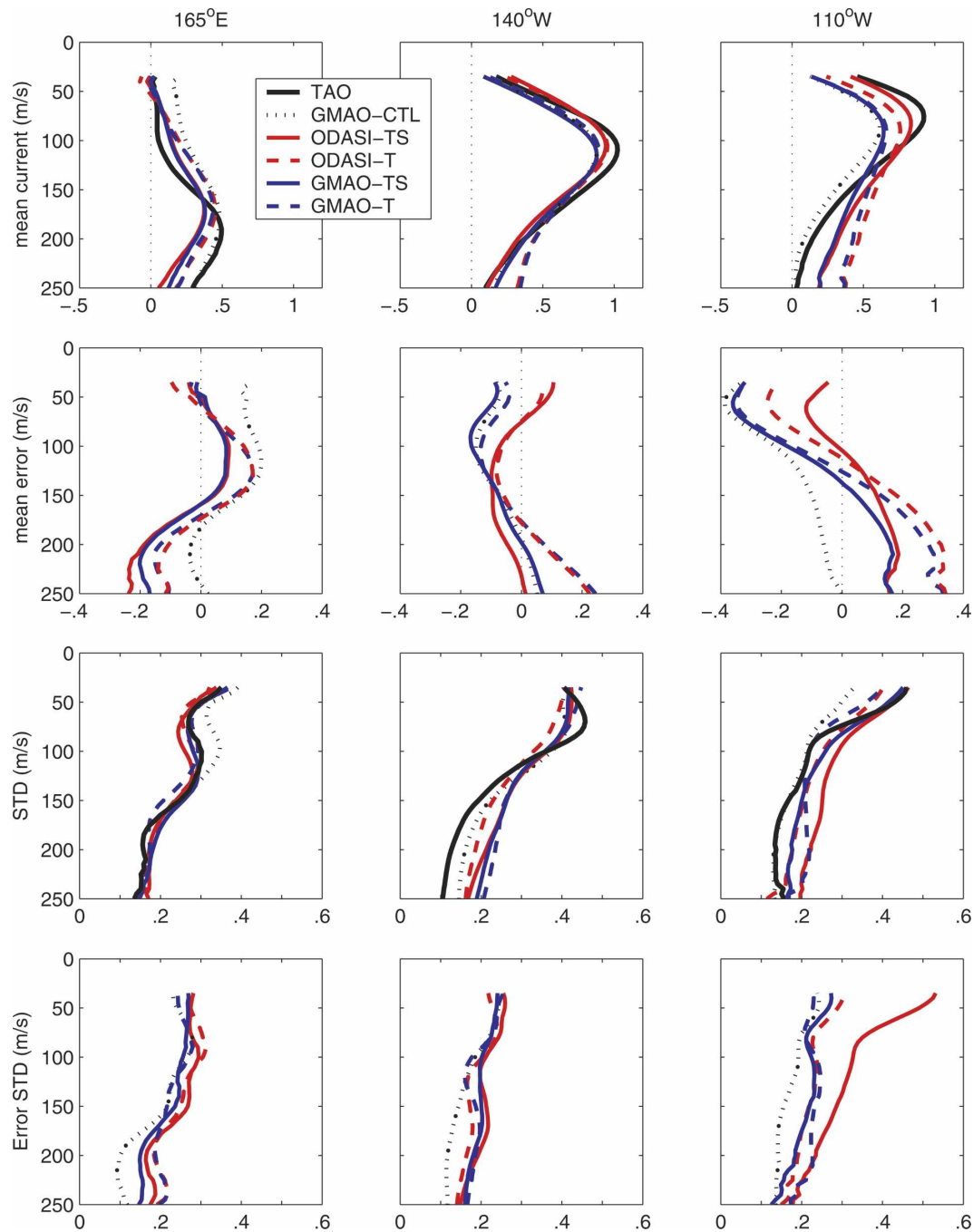
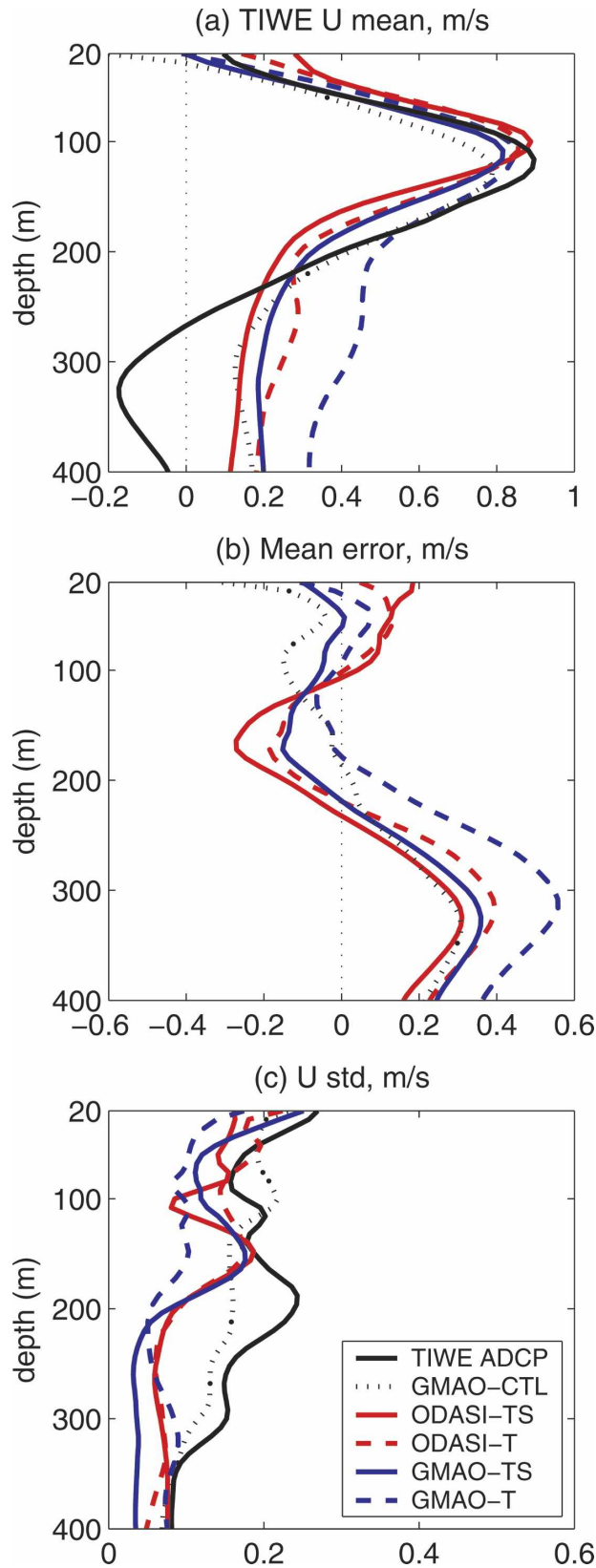


FIG. 12. Same as in Fig. 7, except that the analyses are different: TAO ADCPs (black solid line), ODASI-TS (red solid line), GMAO-TS (blue solid line), ODASI-T (red dashed line), GMAO-T (blue dashed line), and the GMAO-CTL (black dashed line).

induced the downwelling of the eastward-flowing EUC, resulting in an eastward bias below the EUC core. The T scheme, which relies on the model  $T$ - $S$  relationship to adjust salinity, is not capable of correcting the bias in the model salinity field. Ricci et al. (2005) also found that at  $140^\circ$  and  $110^\circ\text{W}$ , the scheme that accounts for

salinity impacts produced smaller eastward bias below the core of EUC as compared to the scheme that does not correct the salinity bias. This suggests that salinity correction is more important at depths that are not directly influenced by surface forcing. Another reason that the salinity adjustments help more at depth is that



the integrated effect of the density gradients grows larger with depth.

*c. Comparison with TIWE cruise ADCP current profiles at 140°W*

During the Tropical Instability Wave Experiment (TIWE) in 1991, two research vessels [Research Vessel (R/V) *Wecoma* and R/V *Monoa Wave*] equipped with shipboard ADCP occupied a station at 140°W on the equator for 38 consecutive days (Lien et al. 1995). These ADCPs measured deeper currents down to about 450 m, usually not available from the moored TAO ADCPs. This provides a rare opportunity to compare the current analysis with independent in situ velocity measurements to deeper depths. We therefore extended GMAO analyses back to 1991 so that a comparison with the TIWE ADCP current observations could be made.

Figure 13 shows the statistics of daily zonal velocity during the TIWE period from the shipboard ADCP, the GMAO-CTL, and the four GMAO analyses. The time mean of the currents is best captured by the GMAO-TS analysis and GMAO-CTL (Fig. 13a). However, the GMAO-CTL has a slight westward bias above 150 m and all analyses and control have an eastward bias below 220 m—none of the model simulations captures the current reversal at that depth. The variability of the in situ measurement below 150 m in this period is generally larger than the four analyses (Fig. 13c), reflecting the fact that the use of a 5-day assimilation period and a 10-day data window, in combination with the IAU, produces a smoothing effect in the analysis that does not capture the high-frequency fluctuations in the current observations. The variability in the GMAO-CTL simulation is relatively closer to the observations below 150 m. Overall, during this time period, the analyses using the TS scheme perform better than the analyses using the T scheme, and the GMAO forcing produces slightly better surface currents than the ODASI forcing.

*d. Comparison with TAO servicing cruises data*

Similar to section 4e, the different GMAO analyses are compared with independent data from the TAO servicing cruises (Fig. 14). All the analyses successfully reduce the temperature error in the model, except that

←

FIG. 13. Zonal current statistics (computed from daily profiles) at 140°W on the equator during the TIWE cruises from 5 Nov to 12 Dec 1991: (a) mean zonal velocity; (b) mean error; and (c) STD of zonal currents.

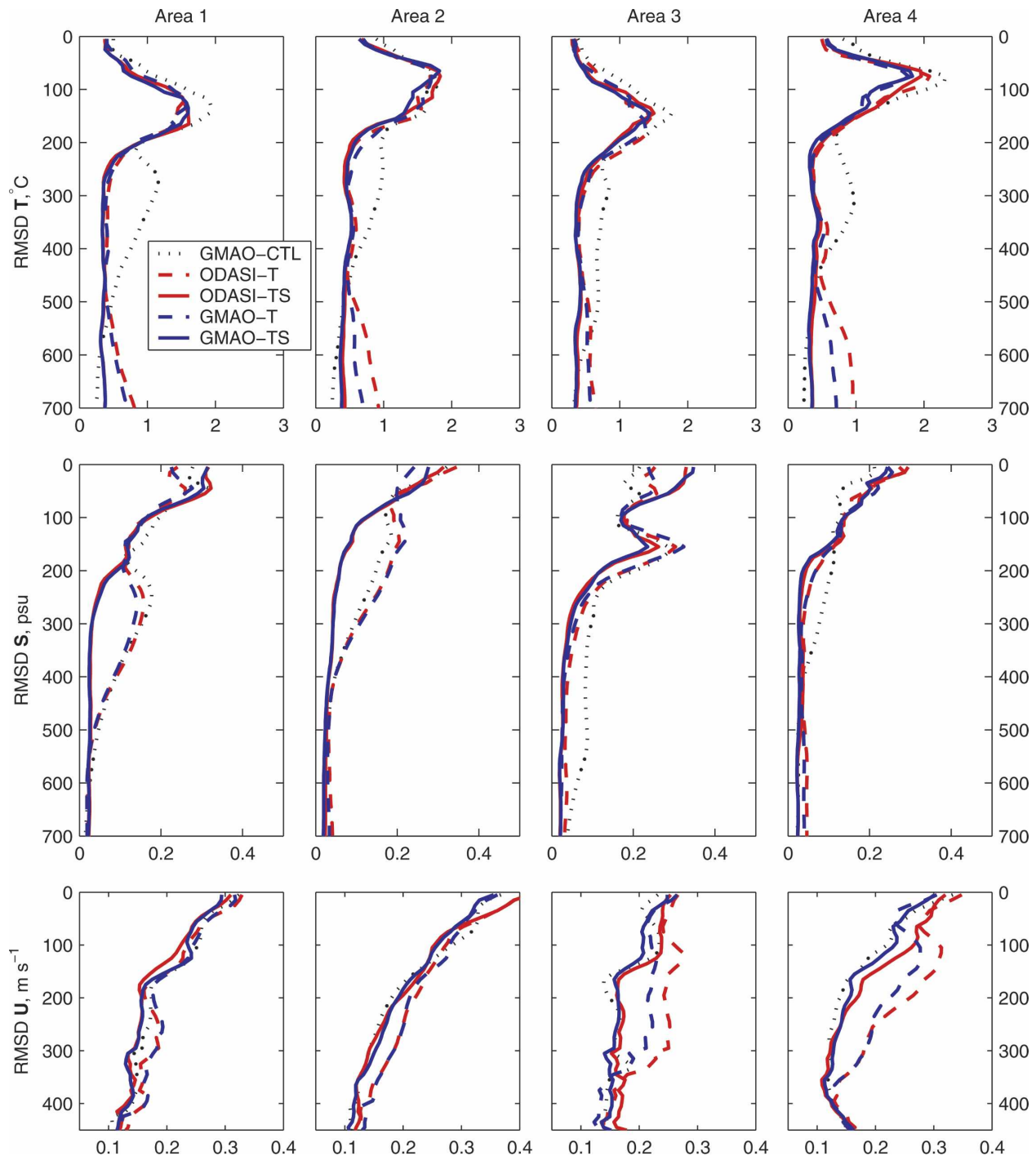


FIG. 14. RMSD of (top) temperature, (middle) salinity, and (bottom) zonal current between model runs and observations from TAO servicing cruises (for the 5-yr period 1994–98) as a function of depth (m), averaged over the northern and southern Niño-3 and Niño-4 regions as shown in Fig. 3.

the T-scheme analyses are worse than the control below 500 m. The reduction of model salinity error by the TS scheme below the thermocline is most prominent in the northern sections of Niño-3 and Niño-4 (areas 1 and 2). The errors in zonal currents are smallest in the GMAO-

TS analysis and GMAO-CTL. ODASI-TS analysis is almost as good except near the surface, which is probably due to slightly larger error in ODASI wind forcing. Both T-scheme analyses have larger errors below the surface in all four regions. As was found from the TAO

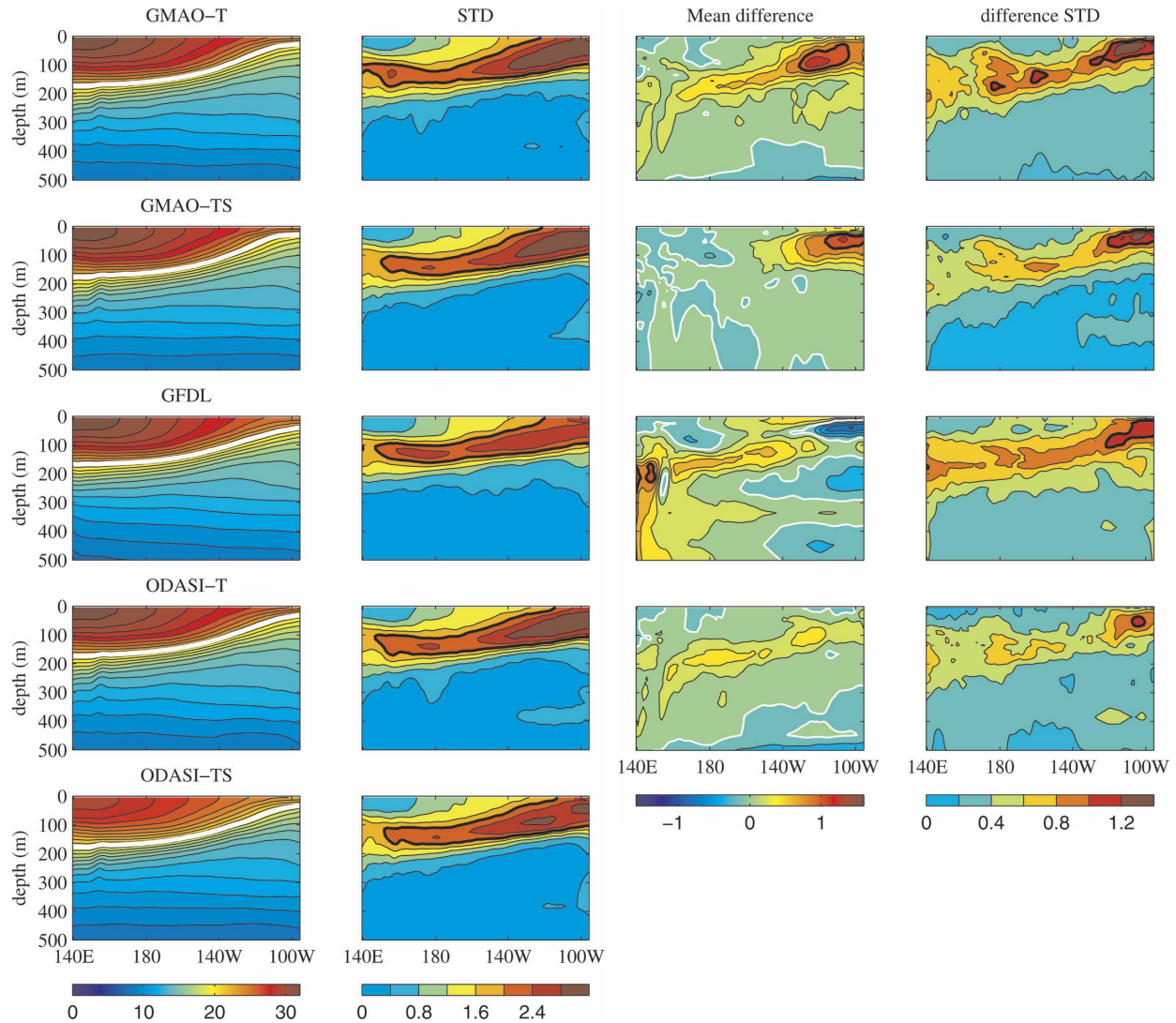


FIG. 15. (left) Mean temperature profiles, (second column) STD of temperature field, (third column) mean difference, and (right) STD of differences of temperature analyses with respect to the ODASI-TS analysis, averaged over the 9-yr period 1993–2001 at the equatorial Pacific section. The thick white contour line in mean state plots is the 20°C isotherm; contour interval (CI) is 1°C. The thick black line in STD plots is the 2°C contour; CI is 0.4°C. The white line in the mean difference plots is the zero contour. In both mean difference and STD of difference plots, the thick black line is the 1°C contour and CI is 0.2°C.

mooring comparison, the TS scheme produces more accurate zonal currents than the T scheme. The T scheme cannot by itself correct model salinity biases. The TS scheme, however, helps to correct model biases and does not appear (from the smaller errors in zonal currents) to disrupt the model balances as much.

*e. Temperature comparison along the equatorial Pacific section*

To get a sense of uncertainty in the temperature analyses across the equatorial Pacific section, we com-

pare three GMAO analyses (GMAO-T, GMAO-TS, and ODASI-T) and the GFDL analysis with the ODASI-TS analysis (i.e., the GMAO analysis that is compared with GFDL analysis in section 4). Figure 15 shows the statistics of the comparisons (to 500-m depth): the time mean and STD of temperature profiles, mean, and standard deviation of the difference of each analysis with respect to the ODASI-TS analysis. The time mean of those analyses under the GMAO forcing are most different from the ODASI-TS analysis near the thermocline (greater than 1°C). These differences are mainly biases with the largest values in the

eastern Pacific (the mean differences are much bigger than the STD of differences in Fig. 15), but they can be significant compared with the variability in the signal (see the STD plots in Fig. 15). Significant differences between GFDL and ODASI-TS analyses extend to the western end of the Pacific and to larger depths. The differences between ODASI-T and ODASI-TS analyses are the smallest above the thermocline. However, note that the differences are the smallest below the thermocline between GMAO-TS and ODASI-TS analyses. This suggests that forcing error is the most important source of error in the temperature analysis above the thermocline, even when temperature observations are assimilated. Below the thermocline, the salinity treatment in the GMAO analyses has a more dominant impact.

## 6. Summary and conclusions

This study evaluates the performance of the GFDL and GMAO ocean analyses in the tropical Pacific with dependent and independent data. The GFDL and GMAO ocean data assimilation systems employ different global ocean circulation models (MOM4 and Poseidon, respectively) and different data assimilation methods (3DVAR and OI, respectively); however, the same forcing and subsurface temperature observation datasets are used by both systems to facilitate their intercomparison (as designed by the ODASI consortium). The GFDL analysis assimilates the temperature profiles only, while the GMAO analysis assimilates a synthetic salinity profile in addition to the temperature profiles. This so-called TS scheme derives a salinity profile for each observed temperature profile based on  $T$ - $S$  relations in the Levitus climatology (Levitus and Boyer 1994). The results show that both GFDL and GMAO analyses reproduce the time mean and variability of the temperature field compared with assimilated TAO temperature data, taking into account the natural variability and representation errors of the assimilated temperature observations. The assimilation of temperature observations also has an impact on the nonobserved state variables, such as salinity and currents. Surface zonal currents at 15 m from the two analyses generally agree with observed climatology from Reverdin et al. (1994) and Bonjean and Lagerloef (2002). Zonal current profiles from the analyses capture the intensity and variability of the Equatorial Undercurrent (EUC) displayed in the independent ADCP data at three TAO moorings across the equatorial Pacific basin. The assimilation of synthetic salinity in the GMAO system significantly reduces the salinity bias, present in both models. Compared with independent data from TAO

servicing cruises, the results show that 1) temperature errors are reduced below the thermocline in both analyses; 2) salinity errors are considerably reduced below the thermocline in the GMAO analysis; and 3) errors in zonal currents from both analyses are comparable. The GFDL current appears to be less sensitive to salinity errors than the GMAO system, probably due to its model's configuration as a z-level OGCM.

To discern the impact of the forcing and salinity treatment, a sensitivity study is undertaken with the GMAO assimilation system. Additional analyses are produced with a different forcing dataset, and another scheme to modify the salinity field is tested. This second scheme updates salinity at the time of temperature assimilation based on model  $T$ - $S$  relationships (denoted "T scheme"; Troccoli and Haines 1999). The results show that both assimilated field (i.e., temperature) and fields that are not directly observed (i.e., salinity and currents) are impacted. Forcing appears to have more impact near the surface (above the core of the Equatorial Undercurrent), while the salinity treatment is more important below the surface that is directly influenced by forcing. Overall, the TS scheme is more effective than the T scheme in correcting model biases in salinity and improving the current structure. Zonal currents from the GMAO control run where no data are assimilated are as good as the best analysis.

In conclusion, both GMAO and GFDL ocean data assimilation systems, using different models and assimilation systems, generate temperature analyses consistent with the observations. The differences are comparable to estimates made of observation representation errors. The assimilation compensates for forcing errors, but differences in forcing products still have a noticeable impact on the near-surface variations. In the GMAO system, assimilating synthetic salinity profiles, deduced from in situ temperature profiles and climatological  $T$ - $S$  relations, is very effective in correcting model bias in salinity and improving the current analysis.

*Acknowledgments.* The authors thank Dave Behringer at NOAA/NCEP and the TAO project at NOAA/PMEL for providing quality-controlled temperature data. Greg Johnson at NOAA/PMEL provided the gridded analyses from TAO servicing cruises. James Moum at Oregon State University and Rien-Chieh Lien at University of Washington provided the TIWE shipboard-ADCP velocity data. Alberto Troccoli implemented the Troccoli-Haines technique with the Poseidon ocean model. Sonya Miller performed the GMAO control runs (forced ocean runs). Anna Borovikov helped with the use of the TAO servicing cruise data. Comments from two anonymous reviewers

helped to improve the presentation of this paper. This research was supported by funding from NOAA/Office of Global Programs, Climate Diagnostics and Experimental Prediction Program, which supported the ODASI collaboration, by the NASA Modeling, Analysis, and Prediction Program under RTOP 622-24-47 and NASA Physical Oceanography Program under RTOP 622-50-01.

## REFERENCES

- Adler, R. F., and Coauthors, 2003: The version-2 Global Precipitation Climatology Project (GPCP) monthly precipitation analysis (1979–present). *J. Hydrometeorol.*, **4**, 1147–1167.
- Alves, O., M. A. Balmaseda, D. Anderson, and T. Stockdale, 2004: Sensitivity of dynamical seasonal forecasts to ocean initial conditions. *Quart. J. Roy. Meteor. Soc.*, **130**, 647–667.
- Atlas, R., R. N. Hoffman, S. C. Bloom, J. C. Jusem, and J. Ardizzone, 1996: A multi-year global surface wind velocity data set using SSM/I wind observations. *Bull. Amer. Meteor. Soc.*, **77**, 869–882.
- Behringer, D., M. Ji, and A. Leetmaa, 1998: An improved coupled model for ENSO prediction and implications for ocean initialization. Part I: The ocean data assimilation system. *Mon. Wea. Rev.*, **126**, 1013–1021.
- Bell, M. J., M. J. Martin, and N. K. Nichols, 2004: Assimilation of data into an ocean model with systematic errors near the equator. *Quart. J. Roy. Meteor. Soc.*, **130**, 873–893.
- Bloom, S. C., L. L. Takacs, A. M. da Silva, and D. Ledvina, 1996: Data assimilation using incremental analysis updates. *Mon. Wea. Rev.*, **124**, 1256–1271.
- Bonjean, F., and G. S. E. Lagerloef, 2002: Diagnostic model and analysis of the surface currents in the tropical Pacific Ocean. *J. Phys. Oceanogr.*, **32**, 2938–2954.
- Borovikov, A., 2005: Multivariate error covariance estimates by Monte-Carlo simulation for oceanographic assimilation studies. Ph.D. thesis, University of Maryland, College Park, 109 pp.
- , M. M. Rienecker, and P. S. Schopf, 2001: Surface heat balance in the equatorial Pacific Ocean: Climatology and the warming event of 1994–95. *J. Climate*, **14**, 2624–2641.
- , —, C. L. Keppenne, and G. C. Johnson, 2005: Multivariate error covariance estimates by Monte Carlo simulation for assimilation studies in the Pacific Ocean. *Mon. Wea. Rev.*, **133**, 2310–2334.
- Burgers, G., M. A. Balmaseda, F. C. Vossepoel, G. J. van Oldenborgh, and P. J. van Leeuwen, 2002: Balanced ocean-data assimilation near the equator. *J. Phys. Oceanogr.*, **32**, 2509–2519.
- Derber, J., and A. Rosati, 1989: A global oceanic data assimilation system. *J. Phys. Oceanogr.*, **19**, 1333–1347.
- Evensen, G., 1994: Sequential data assimilation with a nonlinear quasi-geostrophic model using Monte Carlo methods to forecast error statistics. *J. Geophys. Res.*, **99**, 10 143–10 162.
- , 2003: The ensemble Kalman filter: Theoretical formulation and practical implementation. *Ocean Dyn.*, **53**, 343–367.
- Fevrier, S., and Coauthors, 2000: A multivariate intercomparison between three oceanic GCMs using observed current and thermocline depth anomalies in the tropical Pacific during 1985–1992. *J. Mar. Syst.*, **24**, 249–275.
- Gent, P. R., and J. C. McWilliams, 1990: Isopycnal mixing in ocean circulation models. *J. Phys. Oceanogr.*, **20**, 150–155.
- Gnanadesikan, A., and Coauthors, 2006: GFDL's CM2 global coupled climate models. Part II: The baseline ocean simulation. *J. Climate*, **19**, 675–697.
- Griffies, S., and Coauthors, 2005: Formulation of an ocean model for global climate simulations. *Ocean Sci.*, **1**, 45–79.
- Harrison, D. E., R. D. Romea, and G. A. Vecchi, 2001: Central equatorial Pacific zonal currents. II: The seasonal cycle and the boreal spring surface eastward surge. *J. Mar. Res.*, **59**, 921–948.
- Ji, M., A. Leetmaa, and J. Derber, 1995: An ocean analysis system for seasonal to interannual climate studies. *Mon. Wea. Rev.*, **123**, 460–481.
- , R. Reynolds, and D. W. Behringer, 2000: Use of TOPEX/Poseidon sea level data for ocean analyses and ENSO prediction: Some early results. *J. Climate*, **13**, 216–231.
- Johnson, G. C., M. J. McPhaden, G. D. Rowe, and K. E. McTaggart, 2000: Upper equatorial Pacific Ocean current and salinity variability during the 1996–1998 El Niño–La Niña cycle. *J. Geophys. Res.*, **105**, 1037–1053.
- , B. M. Sloyan, W. S. Kessler, and K. E. McTaggart, 2002: Direct measurements of upper ocean currents and water properties across the tropical Pacific during the 1990s. *Progress in Oceanography*, Vol. 52, Pergamon Press, 31–61.
- Keppenne, C. L., and M. M. Rienecker, 2002: Initial testing of a massively parallel ensemble Kalman filter with the Poseidon isopycnal ocean general circulation model. *Mon. Wea. Rev.*, **130**, 2951–2965.
- , —, N. P. Kurkowski, and D. D. Adamec, 2005: Ensemble Kalman filter assimilation of temperature and altimeter data with bias correction and application to seasonal prediction. *Nonlinear Processes Geophys.*, **12**, 491–503.
- Lagerloef, G. S. E., G. T. Mitchum, R. Lukas, and P. P. Niiler, 1999: Tropical Pacific near surface currents estimated from altimeter, wind, and drifter data. *J. Geophys. Res.*, **104**, 23 313–23 326.
- Large, W. G., J. C. McWilliams, and S. C. Doney, 1994: Oceanic vertical mixing: A review and a model with a nonlocal boundary layer parameterization. *Rev. Geophys.*, **32**, 363–403.
- , G. Danabasoglu, J. C. McWilliams, P. R. Gent, and F. O. Bryan, 2001: Equatorial circulation of a global ocean climate model with anisotropic horizontal viscosity. *J. Phys. Oceanogr.*, **31**, 518–536.
- Levitus, S., and T. P. Boyer, 1994: *Temperature*. Vol. 4, *World Ocean Atlas 1994*, NOAA Atlas NESDIS 4, 117 pp.
- Lien, R.-C., D. R. Caldwell, M. C. Gregg, and J. N. Moum, 1995: Turbulence variability at the equator in the central Pacific at the beginning of the 1991–1993 El Niño. *J. Geophys. Res.*, **100**, 6881–6898.
- Lukas, R., and E. Lindstrom, 1991: The mixed layer of the western equatorial Pacific Ocean. *J. Geophys. Res.*, **96**, 3343–3357.
- Maes, C., J. Picaut, and S. Belamari, 2005: Importance of the salinity barrier layer for the buildup of El Niño. *J. Climate*, **18**, 104–118.
- McPhaden, M. J., and Coauthors, 1998: The Tropical Ocean-Global Atmosphere observing system: A decade of progress. *J. Geophys. Res.*, **103**, 14 169–14 240.
- Murray, R. J., 1996: Explicit generation of orthogonal grids for ocean models. *J. Comput. Phys.*, **126**, 251–273.
- Pacanowski, R., and S. Philander, 1981: Parameterization of vertical mixing in numerical models of the tropical oceans. *J. Phys. Oceanogr.*, **11**, 1443–1451.

- Reverdin, G., C. Frankignoul, E. Kestenare, and M. J. McPhaden, 1994: Seasonal variability in the surface currents of the equatorial Pacific. *J. Geophys. Res.*, **99**, 20 323–20 344.
- Reynolds, R. W., and T. M. Smith, 1994: Improved global sea surface temperature analyses using optimum interpolation. *J. Climate*, **7**, 929–948.
- , N. A. Rayner, T. M. Smith, D. C. Stokes, and W. Wang, 2002: An improved in situ and satellite SST analyses for climate. *J. Climate*, **15**, 1609–1625.
- Ricci, S., A. T. Weaver, J. Vialard, and P. Rogel, 2005: Incorporating state-dependent temperature–salinity constraints in the background error covariance of variational ocean data assimilation. *Mon. Wea. Rev.*, **133**, 317–338.
- Roemmich, D., M. Morris, W. R. Young, and J.-R. Donguy, 1994: Fresh equatorial jets. *J. Phys. Oceanogr.*, **24**, 540–558.
- Rosati, A., K. Miyakoda, and R. Gudgel, 1997: The impact of ocean initial conditions on ENSO forecasting with a coupled model. *Mon. Wea. Rev.*, **125**, 754–772.
- Schopf, P., and A. Loughe, 1995: A reduced-gravity isopycnic ocean model: Hindcasts of El Niño. *Mon. Wea. Rev.*, **123**, 2839–2863.
- Segsneider, J., D. L. T. Anderson, J. Vialard, M. A. Balmaseda, and T. N. Stockdale, 2001: Initialization of seasonal forecasts assimilating sea level and temperature observations. *J. Climate*, **14**, 4292–4307.
- Stammer, D., and Coauthors, 2002: Global ocean circulation during 1992–1997, estimated from ocean observations and a general circulation model. *J. Geophys. Res.*, **107**, 3118, doi:10.1029/2001JC000888.
- Sterl, A., and A. Kattenberg, 1994: Embedding a mixed layer model into an ocean general circulation model of the Atlantic: The importance of surface mixing for heat flux and temperature. *J. Geophys. Res.*, **99**, 14 139–14 157.
- Troccoli, A., and K. Haines, 1999: Use of the temperature–salinity relation in a data assimilation context. *J. Atmos. Oceanic Technol.*, **16**, 2011–2025.
- , and Coauthors, 2002: Salinity adjustments in the presence of temperature data assimilation. *Mon. Wea. Rev.*, **130**, 89–102.
- , M. M. Rienecker, C. L. Keppenne, and G. C. Johnson, 2003: Temperature data assimilation with salinity corrections: Validations for the NSIPP ocean data assimilation system in the tropical Pacific Ocean, 1993–1998. NASA Tech. Memo. 2003-104606, Vol. 24, 23 pp.
- Vialard, J., A. T. Weaver, D. L. T. Anderson, and P. Delecluse, 2003: Three- and four-dimensional variational assimilation with a general circulation model of the tropical Pacific Ocean. Part II: Physical validation. *Mon. Wea. Rev.*, **131**, 1379–1395.
- Vintzileos, A., M. M. Rienecker, M. J. Suarez, S. K. Miller, P. J. Pegion, and J. T. Bacmeister, 2003: Simulation of the El Niño–Southern Oscillation phenomenon with NASA’s Seasonal-to-Interannual Prediction Project coupled general circulation model. *CLIVAR Exchanges*, No. 8, International CLIVAR Project Office, Southampton, United Kingdom, 25–27.
- , —, —, S. Schubert, and S. K. Miller, 2005: Local versus remote wind forcing of the equatorial Pacific surface temperature in July 2003. *Geophys. Res. Lett.*, **32**, L05702, doi:10.1029/2004GL021972.
- Yang, S., K. Lau, and P. Schopf, 1999: Sensitivity of the tropical Pacific Ocean to precipitation induced freshwater flux. *Climate Dyn.*, **15**, 737–750.
- Zhang, S., M. J. Harrison, A. T. Wittenberg, and A. Rosati, 2005: Initialization of an ENSO forecast system using a parallelized ensemble filter. *Mon. Wea. Rev.*, **133**, 3176–3201.